



Kaunas University of Technology
Faculty of Mechanical Engineering and Design

Investigation of the Effect of Abrasive Water Jet Machining Parameters on Fiber-Reinforced Epoxy Composite

Master's Final Degree Project

Sachinkumar Manchery Sajan

Project author

Assoc. Prof. Dr. Kristina Žukienė

Supervisor

Kaunas, 2025



Kaunas University of Technology
Faculty of Mechanical Engineering and Design

Investigation of the Effect of Abrasive Water Jet Machining Parameters on Fiber-Reinforced Epoxy Composite

Master's Final Degree Project
Industrial Engineering and Management (6211EX018)

Sachinkumar Manchery Sajan

Project author

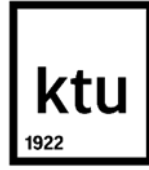
Assoc. Prof. Dr. Kristina Žukienė

Supervisor

Prof. Dr. Daiva Zeleniakienė

Reviewer

Kaunas, 2025



Kaunas University of Technology

Faculty of Mechanical Engineering and Design

Sachinkumar Manchery Sajan

Investigation of the Effect of Abrasive Water Jet Machining Parameters on Fiber-Reinforced Epoxy Composite

Declaration of Academic Integrity

I confirm the following:

1. I have prepared the final degree project independently and honestly without any violations of the copyrights or other rights of others, following the provisions of the Law on Copyrights and Related Rights of the Republic of Lithuania, the Regulations on the Management and Transfer of Intellectual Property of Kaunas University of Technology (hereinafter – University) and the ethical requirements stipulated by the Code of Academic Ethics of the University;
2. All the data and research results provided in the final degree project are correct and obtained legally; none of the parts of this project are plagiarised from any printed or electronic sources; all the quotations and references provided in the text of the final degree project are indicated in the list of references;
3. I have not paid anyone any monetary funds for the final degree project or the parts thereof unless required by the law;
4. I understand that in the case of any discovery of the fact of dishonesty or violation of any rights of others, the academic penalties will be imposed on me under the procedure applied at the University; I will be expelled from the University and my final degree project can be submitted to the Office of the Ombudsperson for Academic Ethics and Procedures in the examination of a possible violation of academic ethics.

Sachinkumar Manchery Sajan

Confirmed electronically



Kaunas University of Technology

Faculty of Mechanical Engineering and Design

Task of the Master's Final Degree Project

Given to the student – Sachinkumar Manchery Sajan

1. Title of the Project

Investigation of the Effect of Abrasive Water Jet Machining Parameters on Fiber-Reinforced Epoxy Composite

(In English)

Abrazyvinio vandens srove atliekamo apdirbimo parametrų įtakos pluoštu armuotiems epoksidiniams kompozitams tyrimas

(In Lithuanian)

2. Aim and Tasks of the Project

Aim: to investigate and compare the effects of abrasive water jet machining parameters on basalt, aramid, carbon, glass fiber reinforced epoxy composite laminates

Tasks:

1. to compare basalt fibre machining process responses with aramid, glass, and carbon fibre reinforced composites, such as top and bottom edge width, edge taper, and surface characteristics;
2. to investigate the optimal machine processing parameters for the texturing of composites: stand-off distance and traverse feed rate;
3. to determine the impact of the machining parameters on the cut cost.

3. Main Requirements and Conditions

To produce FRP composite by the hand lay-up method. Perform the machining experiments on an AWJ machine WAZER Desktop. Achieve the lowest possible values of R_a , R_q , and delamination damage when cutting through an abrasive water jet of fiber-reinforced polymer composite material manufactured in $[0^\circ/90^\circ]_5$ fabric orientation. The main parameters to be studied are the stand-off distance and the feed rate.

4. Additional Requirements for the Project, Report and its Annexes

“Not applicable”

Project author	Sachinkumar Manchery Sajan	07-03-2025
	<i>(Name, Surname)</i>	<i>(Date)</i>
	<i>(Signature)</i>	
Supervisor	Kristina Žukienė	07-03-2025
	<i>(Name, Surname)</i>	<i>(Date)</i>
	<i>(Signature)</i>	
Head of study field programs	Regita Bendikienė	07-03-2025
	<i>(Name, Surname)</i>	<i>(Date)</i>
	<i>(Signature)</i>	

Manchery Sajan Sachinkumar. Investigation of the Effect of Abrasive Water Jet Machining Parameters on Fiber-Reinforced Epoxy Composite. Master's Final Degree Project, supervisor Assoc. Prof. Dr. Kristina Žukienė; Faculty of Mechanical Engineering and Design, Kaunas University of Technology.

Study field and area (study field group): Production and Manufacturing Engineering (E10), Engineering Sciences (E).

Keywords: composite; abrasive water jet; cutting; roughness; Kerf; surface texturing.

Kaunas, 2025. 55 p.

Summary

Today, there are advanced modern cutting methods available on the market for a wide range of materials, which help industrial companies to solve many material processing problems, such as very high cutting precision, designing more complex profiles, significantly reducing production time, and minimizing the amount of waste generated during production. Various composite materials are also now widely used due to the excellent properties of composite materials, such as flexibility in design, low density, high strength, and long-term durability. There is also a wide range of processing techniques for composite materials. Of these methods, abrasive water jet machining is one of the most popular and best methods offered by researchers due to the quality of the output it provides. This project presents a study of abrasive water jet machining (AWJM) of four types of fibre reinforced polymer composites, such as basalt, glass, carbon, and aramid. The abrasive water jet cut and texture quality of these fibre-reinforced composite laminates have been investigated by analysing various parameters such as surface roughness values, kerf width, and angle. The results of the experiment confirm that cutting composite materials using AWJM ensures high quality and precision. The influence of two different feed speeds (fine 50 mm/s and coarse 70 mm/s) on cutting quality was investigated and showed good machining results for all composite materials. With the exception of the carbon fibre reinforced epoxy composite, delamination was observed in all other fibre reinforced epoxy composites, which is very common in machining composites. From the cutting angles and surface roughness values, it was found that fine cutting provides better quality than coarse cutting. The analysis of the texturing results showed that only carbon and aramid fibre reinforced epoxy resin composites could be textured using predefined machining parameters. The cutting cost calculations show that coarse cutting is much more economical than fine cutting. This can reduce the environmental impact by reducing operating costs and waste after the machining process.

Manchery Sajan Sachinkumar. Abrazyvinio vandens srove atliekamo apdirbimo parametrų įtakos pluoštu armuotiems epoksidiniams kompozitams tyrimas. Magistro baigiamasis projektas / vadovė doc. dr. Kristina Žukienė; Kauno technologijos universitetas, Mechanikos inžinerijos ir dizaino fakultetas.

Studijų kryptis ir sritis (studijų krypčių grupė): Gamybos inžinerija (E10), Inžinerijos mokslai (E).

Reikšminiai žodžiai: kompozitas; vandens-abrazyvo srovės pjovimo staklės; pjovimas; šiurkštumas; kerfas; paviršiaus tekstūravimas.

Kaunas, 2025. 55 p.

Santrauka

Šiandien rinkoje yra pažangių šiuolaikinių įvairių medžiagų pjovimo metodų, kurie padeda pramonės įmonėms išspręsti daugelį medžiagų apdirbimo problemų, pvz., labai didelį pjovimo tikslumą, projektuoti sudėtingesnius profilius, gerokai sutrumpinti gamybos laiką ir sumažinti gamybos metu susidarančių atliekų kiekį. Įvairios kompozicinės medžiagos dabar taip pat plačiai naudojamos dėl puikių kompozitinių medžiagų savybių, tokių kaip lankstumas projektuojant, mažas tankis, didelis stiprumas ir ilgalaikis patvarumas. Be to, yra daug įvairių kompozitinių medžiagų apdirbimo būdų. Iš šių metodų abrazyvinio vandens srove atliekamas apdirbimas (AWJM) yra vienas populiariausių ir geriausių siūlomų metodų dėl gaunamos produkcijos kokybės. Šiame projekte pateikiamas keturių rūšių pluoštu armuotų epoksidinės dervos kompozitų, tokių kaip bazaltas, stiklas, anglis ir aramidai, AWJM tyrimas. Šių pluoštu armuotų kompozitų laminatų AWJ pjūvio ir tekstūros kokybė buvo tiriama analizuojant įvairius parametrus, tokius kaip paviršiaus šiurkštumo vertės, briaunos plotis ir kampas. Eksperimento rezultatai patvirtina, kompozitinių medžiagų pjovimas, naudojant AWJM, užtikrina aukštą kokybę ir tikslumą. Darbe buvo tiriama dviejų skirtingų pastūmos greičių (smulkus 50 mm/s ir stambus 70 mm/s) įtaka pjovimo kokybei parodė gerus visų kompozitinių medžiagų apdirbimo rezultatus. Išskyrus anglies pluoštu armuotą epoksido kompozitą, visais kitais pluoštais armuotose epoksidiniuose kompozituose, buvo pastebėtas išsisluoksniavimas, kuris labai dažnas apdirbant kompozitus. Iš pjovimo kampų ir paviršiaus šiurkštumo verčių nustatyta, kad smulkusis pjovimas užtikrina geresnę kokybę nei stambusis. Išanalizavus tekstūravimo rezultatus, nustatyta, kad tik anglies ir aramido pluoštais armuotus epoksidinės dervos kompozitus buvo galima tekstūruoti naudojant iš anksto nustatytus mašinos apdirbimo parametrus. Pjovimo sąnaudų skaičiavimai rodo, kad stambus pjovimas yra daug ekonomiškė nei smulkus. Tai gali sumažinti poveikį aplinkai, nes sumažėja eksploatacinės išlaidos ir atliekos po apdirbimo proceso.

Table of Contents

List of Figures	8
List of Tables.....	9
List of Abbreviations and Terms	10
Introduction	11
1. Composite Materials and Cutting Methods	12
1.1. Composite Materials.....	12
1.2. Cutting Methods	13
1.2.1. Laser Cutting Method.....	14
1.2.2. Abrasive Water Jet Machine	14
1.2.3. Diamond Cutting	15
1.3. Cutting Defects in Composites.....	16
1.3.1. Cutting Defects of AWJM.....	17
1.4. AWJ Cutting Quality.....	19
1.4.1. Geometric Variations on Cut Surfaces	19
1.4.2. Kerf Angle.....	20
1.4.3. Surface Roughness	21
1.5. Texturing of Composites	22
1.6. Chapter Summary	24
2. Materials and Experimentation	25
2.1. Materials.....	25
2.2. Preparation of Composite Laminates	25
2.3. Cutting of Samples Using AWJM.....	26
2.4. Surface Roughness Analysis Using ImageJ Software.....	27
2.5. Kerf Angle Measurement	28
2.6. Texturing on Composites	28
2.7. Chapter Summary.....	28
3. Comparison of Processing Reactions of Basalt Fibre-Reinforced Composites with Aramid, Glass, and Carbon Fibre-Reinforced Composites	29
3.1. Quality of Cut Samples	29
3.2. Surface Roughness Analysis	33
3.3. Kerf Angle Value	39
3.4. Texturing On Composites.....	41
3.5. Kerf Angle Calculation of Texturing	46
3.6. Cutting Cost Calculation	47
3.7. Chapter Summary	48
4. Environmental and Economic Impacts of the Application of AWJM.....	49
4.1. Environmental Impacts.....	49
4.2. Economic Impacts	49
4.3. Chapter Summary	50
Conclusions	51
List of References.....	52
Appendices	56

List of Figures

Fig. 1. Laser cutting (a) illustration of CO ₂ laser, (b) actual laser cutting setup [8]	14
Fig. 2. Scanning electron microscope image of garnet particles [11]	15
Fig. 3. AWJM schematic diagram [12]	15
Fig. 4. Diamond cutting (a) schematic and (b) experimental laser-assisted diamond cutting setup [13]	16
Fig. 5. Defects in the form of pulled fibers are indicated by arrows [21]	16
Fig. 6. Defects in the form of tron fibers indicated by arrows [21].....	16
Fig. 7. Matrix chipping fibers indicated by arrows [21]	17
Fig. 8. Chipping occurring at the interface between the matrix and fibers is indicated by arrows [21]	17
Fig. 9. Delamination mechanism during AWJM: (a) fracture initiation, (b) water-wedging, and (c) abrasive embedment [27].....	18
Fig. 10. Abrasive particles embedded between the laminates [27]	19
Fig. 11. Different phenomena observed on cut surfaces [30]	19
Fig. 12. Kerf plot geometry [34]	20
Fig. 13. Energy distribution of water jet from the nozzle to the material surface [36]	20
Fig. 14. Ra and Rq values [38].....	21
Fig. 15. Laser texturizing results (a) dimples and (b) grooves [43]	22
Fig. 16. Schematic for micro-texturing of polymer using the laser beam [43]	22
Fig. 17. Electrochemical machining [45]	23
Fig. 18. AWJM is used for repairing the CFRP in the aerospace industry [46]	23
Fig. 19. Vacuum bagging	25
Fig. 20. Cutting direction of samples	26
Fig. 21. <i>Wazer Desktop</i> AWJM.....	26
Fig. 22. Optical microscope ECLIPSE LV100ND_Nikon	27
Fig. 23. The profilogram of the BFRPC surface after cutting (a) coarse, (b) fine	33
Fig. 23. The profilogram of the BFRPC surface after cutting (a) coarse, (b) fine	34
Fig. 24. The profilogram of the AFRPC surface after cutting (a) coarse, (b) fine.....	35
Fig. 25. The profilogram of the CFRPC surface after cutting (a) coarse, (b) fine	36
Fig. 26. The profilogram of the GFRPC surface after cutting (a) coarse, (b) fine.....	37
Fig. 27. Surface roughness values of composite samples with cutting type	38
Fig. 28. Kerf taper angle values of BFRPC samples, coarse cutting (70mm/s) (a) and fine cutting (50 mm/s) (b) with 1.3× magnification.....	39
Fig. 29. Kerf taper angle values of CFRPC samples, coarse cutting (70mm/s) (a) and fine cutting (50 mm/s) (b) with 1.3× magnification.....	40
Fig. 30. Kerf taper angle values of AFRPC samples, coarse cutting (70 mm/s) (a) and fine cutting (50 mm/s) (b) with 1.3× magnification.....	40
Fig. 31. Kerf taper angle values of GFRPC samples, coarse cutting (70 mm/s) (a) and fine cutting (50 mm/s) (b) with 1.3× magnification.....	40
Fig. 32. Kerf taper angle values of composite samples with cutting type.....	41
Fig. 33. CFRPC sample with cuts of feed rates of 300 mm/s and 350 mm/s.....	43
Fig. 34. AFRPC sample with cuts of feed rates of 300 mm/s and 350 mm/s	43
Fig. 35. BFRPC sample with cuts of feed rates of 300mm/s and 350mm/s.....	44
Fig. 36. GFRPC sample with cuts of feed rates of 300 mm/s and 350 mm/s	44

List of Tables

Table 1. Composites, qualities, and applications.....	13
Table 2. Cutting and electrical parameters of <i>Wazer Desktop AWJM</i>	27
Table 3. Images of cut samples of composites for coarse and fine cutting	30
Table 4. Delamination on BFRPC, AFRPC, and GFRPC samples, coarse cutting (e) and fine cutting (f)	31
Table 5. Optical microscope images of composite cross-sections of coarse and fine cutting	32
Table 6. Materials and the surface roughness values.....	38
Table 7. Texturing on composite samples in different SOD and feed rate.....	42
Table 8. Texturing effect for composites increasing feed rate with constant SOD (2.28mm SOD)	42
Table 9. Texturing effect for composites increasing SOD with constant feed rate (250mm/s).....	43
Table 10. Values of the upper and lower kerf width of AFRPC for increasing feed rate at 2.28mm SOD	44
Table 11. Values of the upper and lower kerf width of AFRPC for increasing SOD at constant feed rate	45
Table 12. Values of the upper and lower kerf width of CFRPC for increasing feed rate at 2.28mm SOD	45
Table 13. Values of the upper and lower kerf width of CFRPC for increasing SOD at constant feed rate	45
Table 14. Values of the upper and lower kerf width of GFRPC for increasing feed rate at 2.28mm SOD	45
Table 15. Values of the upper and lower kerf width of GFRPC for increasing SOD at constant feed rate	45
Table 16. Values of the upper and lower kerf width of BFRPC for feed rate at constant SOD	45
Table 17. Values of the upper and lower kerf width of BFRPC for increasing SOD at constant feed rate	46
Table 18. Texturing effect for composites increasing feed rate at constant SOD	46
Table 19. Texturing effect for composites increasing SOD at constant feed rate	46
Table 20. Cutting cost.....	47

List of Abbreviations and Terms

Abbreviations:

AFRPC – aramid fiber reinforced polymer composite

GFRPC – glass fiber reinforced polymer composite

CFRPC – carbon fiber reinforced polymer composite

BFRPC – basalt fiber reinforced polymer composite

SOD – stand of distance (mm)

AWJM – abrasive water jet machining

SiCp/Al – silicon carbide particle-reinforced aluminum matrix composites

R_a – arithmetic average roughness (μm)

R_q – root mean squared roughness (μm)

W_t – top kerf width (mm)

W_b – bottom kerf width (mm)

t – thickness (mm)

Introduction

Composite materials are increasingly used in all industries around the world today. Composites are made by mixing two materials with different properties to create a desired material with unique properties that the individual materials do not have. Composite materials are used in all industries, such as aerospace, automotive, renewable energy, sports, electronics, and construction. In recent years, composites have revolutionized the industry as they have properties that natural materials cannot offer, such as high strength, durability, etc. The production of composites from natural materials is very popular now due to the sustainability advantages. A good example of this is basalt, which is made by melting down basalt rock and turning it into fibers. As with all other composite materials, the main advantages of basalt are that it is lightweight, environmentally friendly, durable, and very strong. The processing of composite materials also plays a major role in industries. There are many different methods for processing these materials, such as laser cutting, water jet cutting, and diamond machining. Of these processes, abrasive waterjet (AWJ) machining is of greater importance due to the quality and many advantages that waterjet cutting can offer. AWJ machining can be used for cutting a wide variety of materials, ranging from wood to composites. Not only cutting but also AWJM is useful for some machining processes such as milling and drilling. Many defects occur during the machining process, such as delamination, fiber extraction from the material, and poor cut quality. All these defects make it difficult to achieve the desired result with modern machining methods. Therefore, it is important to evaluate the cutting quality of modern cutting methods for composite materials. This paper discusses the application of AWJ machining on various fiber-reinforced epoxy composites, i.e., basalt, glass, carbon, and aramid. The focus is on the influence of AWJ cutting parameters on the cutting quality of these composites. The possibilities of texture formation with AWJ are also investigated.

Aim: to investigate and compare the effects of abrasive water jet machining parameters on basalt, aramid, carbon, glass fiber reinforced epoxy composite laminates.

Tasks:

1. to compare basalt fibre machining process responses with aramid, glass, and carbon fibre reinforced composites, such as top and bottom edge width, edge taper, and surface characteristics;
2. to investigate the optimal machine processing parameters for the texturing of composites: stand-off distance and traverse feed rate;
3. to determine the impact of the machining parameters on the cut cost.

Hypothesis: To ensure high machining quality, it is necessary to select different AWJ machining parameters for different types of fiber-reinforced composites.

1. Composite Materials and Cutting Methods

Modern technology requires highly advanced and quality materials to fulfill the needs and demands of technological progress in the industries. One of the modern materials that meets these criteria is composites. The special and unique combination of material properties makes this material more important. The main advantages of composite materials are that they have better properties than conventional materials, e.g., strength, durability, deformation, etc. [1]. Among these composites, composites consisting of components of natural origin have greater importance due to their low production or market cost and sustainability due to their environmentally friendly character.

Due to their high quality, composites are used in many industries today. At the same time, the processing, machining, and repairing of composites is very important to achieve great results without compromising the material quality. Some examples of cutting processes for composite materials are Abrasive waterjet cutting is used for strong materials such as composite materials, laser cutting for thick materials and diamond cutting for stone, especially marble.

Abrasive waterjet cutting (AWJM) is an advanced, modern material processing technology that uses powerful water jets which mixed with abrasive particles. The most commonly used abrasive particles are alumina or garnet. The presence of abrasive particles with a high speed of the water jet stream makes it possible to remove the material from the workpiece and thus precisely process the surface, e.g., for cutting or shaping [2,3]. In the aerospace industry, AWJM is one of the most commonly used processes due to the improved properties of composite materials. The chances of damage to composite materials are very common in the aerospace industry due to different physical and environmental conditions. Therefore, repairing these parts is essential, and processing these composites using conventional methods leads to thermal and mechanical damage, which has an even greater negative impact on the mechanical properties [3]. In addition, the right choice of process parameters is crucial to achieve the desired result.

1.1. Composite Materials

Composite materials are a type of material mainly made up of two parts, a reinforcement part and a matrix part. In the markets, there is a wide variety of composites available based on the materials used to make them. Based on the reinforcement fiber used in a composite, it can be divided into different categories. Carbon fiber reinforced polymer composites (CFRPC), aramid fiber reinforced polymer composites (AFRPC), and glass fiber reinforced polymer composites (GFRPC) are examples of composites. Some examples of metal matrix composites are Aluminum matrix composites and titanium matrix composites [4]. The composites have great strength and stiffness mechanical qualities from these materials. Not only fibers and metals, but also, there are composites with natural fibers like basalt and nanoparticles. One of the great examples of a synthetic matrix that can provide better qualities to a composite is Epoxy resin for the production of composites [4].

The use of composite materials is well known in various industries for their excellent properties. The use of CFRPC in the aircraft industry is a great example of this. They are mainly used for the production of parts in the aircraft industry [4]. Many body parts of aircraft are made from CFRPC because it is a very lightweight material and helps the aircraft to achieve better fuel efficiency [4]. In addition, due to the same properties, this material is also used in the production units of cars as it helps them to achieve higher speeds with high body strength with light weight. Another example is that, due to its high resistance to environmental damage, composites with glass fibers are used in the

marine industry [5]. The quality of GFRPC to withstand damage due to impact loads makes it an important material in the marine industry. They also have very good specific strength and stiffness. Composites with aramid fiber are also well known in the military, aerospace, and sports industries [6]. Table 1 lists some of the main properties and applications of the fibers used in the experimental part of this work. The table shows that almost all composites have the same properties and market applications.

Table 1. Composites, qualities, and applications

Composite	Main Qualities	Main Applications
AFRPC	Major quality is very high resistance to impact, low weight, and it does not conduct electricity	Main usage is in the military for making armor like bulletproof vests and helmets, also used in aerospace and automobiles for making parts.
GFRPC	Low price is the main quality with low weight and high strength. Resistant to corrosion also.	Due to its low price, it is used in almost every industry, including military, telecommunication, sports etc.
CFRPC	High strength and stiffness, low weight compared to other composites, and resistance to corrosion, also	In Aerospace for body parts, Marine, Automotive parts, also made from CFRPC, in the Renewable energy industry for wind turbines
BFRPC	The main quality is that it is environmentally friendly, making it more attractive, resistant to many things like chemicals and corrosion.	It is also used in many industries due to its quality of being environmentally friendly, such as construction, renewable energy, and automobile, etc.

The production of composites from natural fibers has become very important nowadays due to the harmful effects caused by the waste of composites after their use and during the machining operations. The recycling of composite waste is a major issue in industries due to the huge application of composites for different purposes. For this reason, natural fibers are gaining importance day by day as they are very eco-friendly and the cost of production is much lower than compared of other composite materials. Among these, basalt fibers have seen more importance in recent years due to their good mechanical, thermal, and chemical properties [7]. The basalt fibers are made from the volcanic rock called basalt, which gives it that name. The cooling and solidification process of molten lava results in these rocks. Silica is the main chemical constituent of basaltic rocks, and the percentage of this oxide depends on the geographical location in which these rocks occur [7]. One of the qualities of Basalt fibers is that the rate of fiber, when compared with its quality, is cheap, which helps manufacturers to reduce the production cost of these fibers without compromising the quality of the fibers [7].

1.2. Cutting Methods

Composite cutting is a complicated process because it can result in numerous defects, risks, and errors. But in the market, there are numerous methods available only for cutting composite materials, such as waterjet cutting, laser cutting, plasma cutting, abrasive cutting, etc. [8]. The major disadvantage of conventional methods is that the processing of these techniques is not as easy as modern methods[8]. At the same time, laser cutting and AWJ cutting, like modern technologies, are very strong in terms of quality provided and process cost efficiency. Laser cutting is widely used in industries due to the non-contact character of the method, but it is a thermally dependent process. The major advantages of laser cutting are operation of this machine is comparatively easy, low waste

production compared to traditional methods, noiselessness compared to traditional methods, high accuracy in cutting, etc. [8]. At the same time, due to the numerous variables that control the process in laser cutting making it is more complicated compared to AWJM. Therefore, due to the competition in the market, the companies that manufacture laser cutting machines are trying their best to improve the ease of controlling and the quality of the machines. Compared to laser technology, waterjet cutting machines are much easier to handle and less expensive [8].

1.2.1. Laser Cutting Method

Laser cutting is a method based on the thermal cutting setup, which can be used for a wide variety of materials, including composites [8]. The main qualities of laser cutting are minimal waste production and durability of the method. In addition, the ease of use of the machine and the very high precision in machining processes [8]. The popularity of this method in the industry is due to the high-quality machining and cost-effectiveness during a large number of processes [9]. Fig. 1 represents a laser cutting machine setup. Compared to AWJM, laser cutting is much faster in terms of working and material removal [10]. One of the major issues related to laser cutting is the production of a heat-affected zone during the operations. It is inevitable in the case of laser cutting compared to AWJM [10].

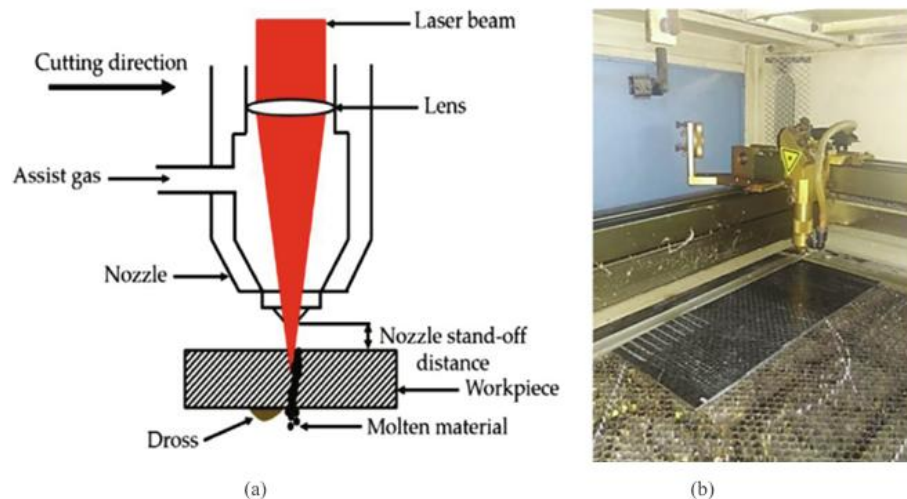


Fig. 1. Laser cutting (a) illustration of CO₂ laser, (b) actual laser cutting setup [8]

1.2.2. Abrasive Water Jet Machine

AWJ cutting is one of the advanced cutting methods for materials to solve problems related to machining different engineering materials. AWJM is a method that combines water jets and solid particles in a proper proportion to cut materials. Fig. 3 shows the schematic diagram of AWJM. AWJM is a single-unit machine that is composed of different parts to complete the machining or cutting action [11]. AWJM is very popular among modern methods because it does not produce a heat-affected zone after cutting the workpiece. Adding abrasive particles to the water jet will help the machine make the cutting process easier and more accurate [11]. Fig. 2 shows the scanning electron microscopic image of garnet particles used for AWJM. The common abrasive particle used in AWJM is garnet because of its high hardness and sharp edges, which help for effective cutting, are more environmentally friendly, and are also available in various mesh sizes. The selection of the abrasive also depends on the workpiece used for the cutting operation. It is hard to identify the better abrasive

for specially designed materials with a mix of different components [11]. Although AWJM is one of the best methods available, there are some issues related to this method, such as the tapering associated with the cutting kerf. The outcome of AWJM is evaluated on the kerf angles, rate of material removal, and surface roughness analysis [12].

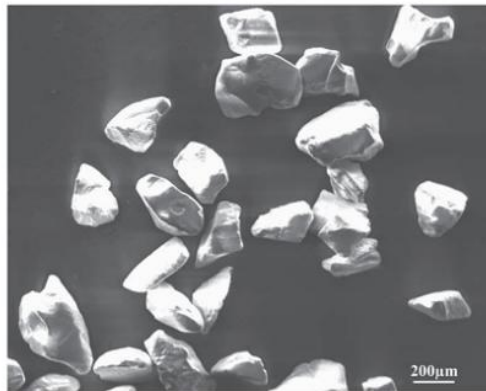


Fig. 2. Scanning electron microscope image of garnet particles [11]

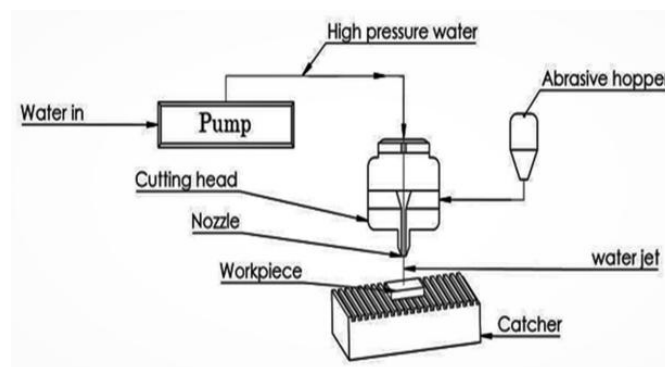


Fig. 3. AWJM schematic diagram [12]

1.2.3. Diamond Cutting

Among the popular methods of composite cutting, diamond cutting is the least used method these days because of the high cost and tool wear. Although for some applications, such as the machining of silicon carbide particle-reinforced aluminum matrix (SiCp/Al) composites, researchers used the laser-assisted diamond cutting method [13]. Diamond cutting was very popular as an ultra-precision method due to very good precision, surface finish, and good removal rate of materials, etc. [13]. Using a diamond cutting method assisted with laser cutting results in surface defects and improves the quality of the surface [13]. Composites like SiCp/Al are widely used for several applications in industries such as military, automobile, and aerospace [14]. Using conventional methods, it is very difficult to achieve a good quality of surface after machining because the mix of SiC particles and aluminium matrix results in very poor machinability [15, 16]. From the investigation of diamond cutting for SiCp/Al composites, it is clear that during this method, the pull-out and fracture of SiC particles occurred [17]. Moreover, some other defects also occurred, such as pits and cracks on the surface after machining. [18]. The quality of the surface and the size of SiCp/Al particles are closely related. Quality decreases with increasing particle size [18]. Laser-assisted machining has some

advantages, such as improving surface quality and reducing surface defects [19]. Fig. 4 shows the schematic and experimental setup of laser laser-assisted diamond cutting setup.

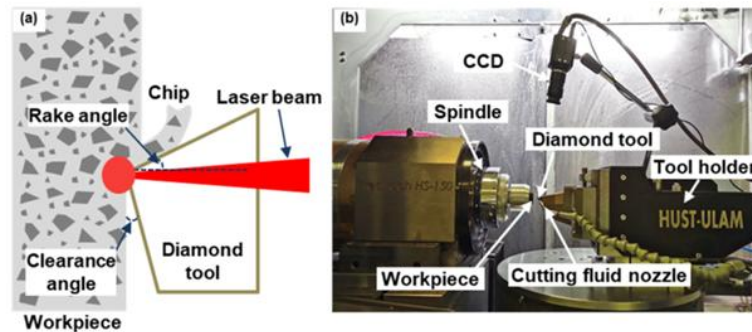


Fig. 4. Diamond cutting (a) schematic and (b) experimental laser-assisted diamond cutting setup [13]

1.3. Cutting Defects in Composites

Cutting of composite can result in many defects, and this can prevent the surface from desired results. Defects in composites can be due to any reason, such as from the production time or it can be from the machining time. The presence of defects during the production time can enhance the chance of defects occurring in composites [20]. The major locations in composites where the defects can happen are the matrix and the fiber. The fiber part is associated with defects such as delamination, fiber pull out, and breakage of fiber, whereas the matrix faces defects such as chipping, deformation of matrix, and thermal degradation. Figs. 5 and 6 show the microscopical observation of defects on the fiber, called fiber pull-out and torn fiber [21].

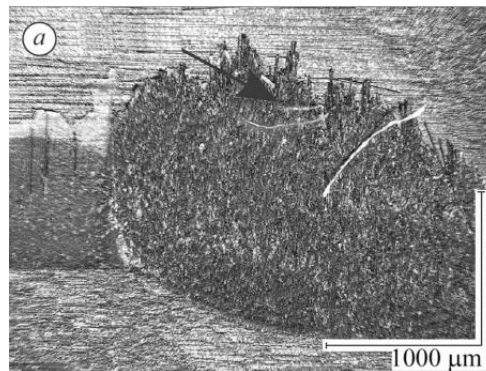


Fig. 5. Defects in the form of pulled fibers are indicated by arrows [21]

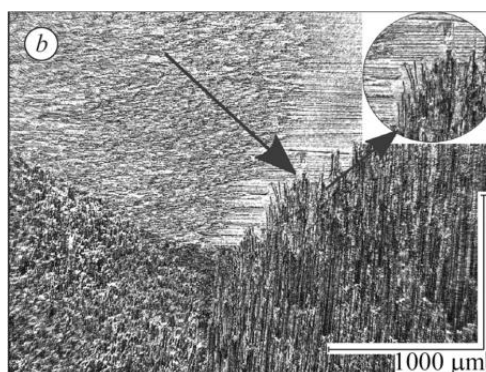


Fig. 6. Defects in the form of tron fibers indicated by arrows [21]

Pulled fiber in Fig. 5 is the most common defect in composites. It happened because during the milling operation, reinforced fibers may undergo tearing. Another important defect is the matrix chipping and chipping on the interface between the matrix and fiber. Fig. 7 shows the matrix chipping defect occurring in composites during the machining operation. And Fig. 8 shows the same chipping between the fiber and matrix interface [21]. Not only these defects there is one more very common defect with the machining of composites is delamination. This defect is very common in almost every cutting method of composites. The values of machining parameters are very important in the case of defects since those parameters have a huge impact on determining the surface roughness and defects on the surface [22,23,24]. There are some methods available for removing the defects, such as brushing and machining. This method can be used for removing defects like scratches. A study about this method shows that low forces in the process of brushing make it possible to remove the defects [25].

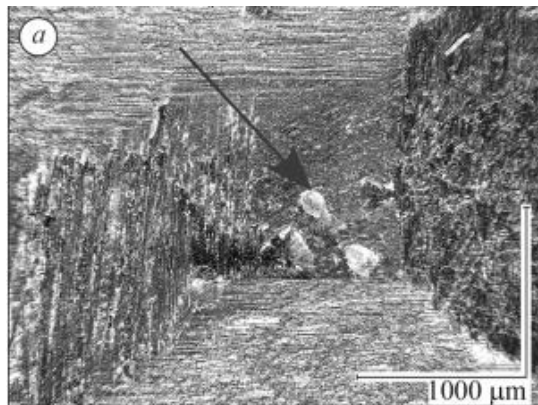


Fig. 7. Matrix chipping fibers indicated by arrows [21]



Fig. 8. Chipping occurring at the interface between the matrix and fibers is indicated by arrows [21]

1.3.1. Cutting Defects of AWJM

All cutting methods have their advantages and disadvantages. Compared to conventional methods, modern cutting methods such as laser cutting and water jet cutting are more convenient and energy-saving [26]. The major problem faced with composites machining is the delamination occurring during the process [27]. This can be avoided up to a certain limit by the use of modern methods. Due to the limitless possibilities for making different composites, finding a convenient and proper method for cutting is also very important. Mistaken methods can result in delamination, cracking of the edges,

and loss of its properties [27]. The quality of composite materials plays a vital role in the aviation industry for the durability and safety of aircraft. Not only in the aviation industry but also in all industries where composite materials are used [27].

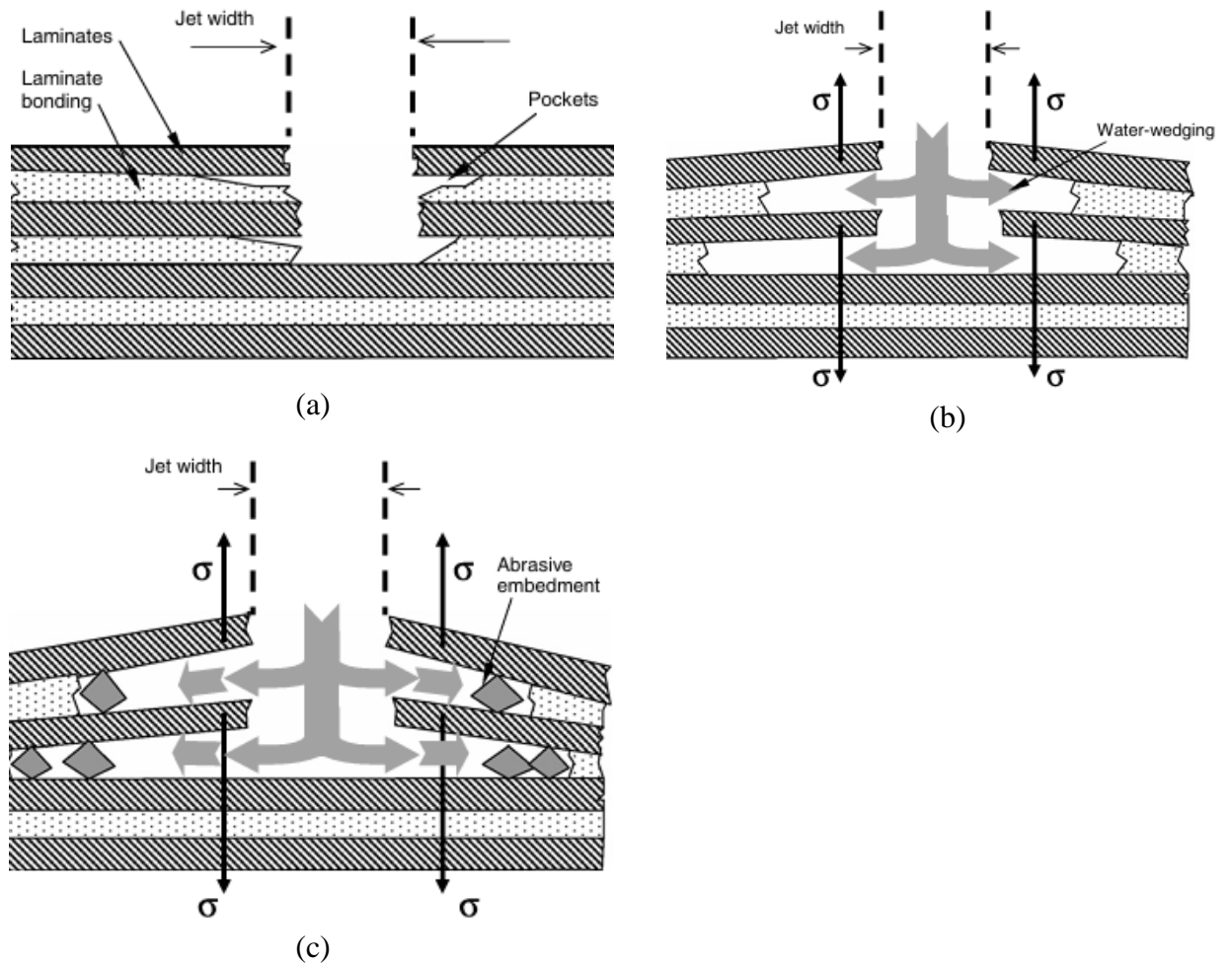


Fig. 9. Delamination mechanism during AWJM: (a) fracture initiation, (b) water-wedging, and (c) abrasive embedment [27]

Fig. 9 shows the different stages of the delamination mechanism during the cutting operation using AWJM. There are multiple reasons for delamination in AWJM. Fracture initiation is the initial stage of delamination, where the water jet hits the workpiece and creates small cracks in the fiber laminates. During the further process, the water jet enters the laminates' cracks and results in water wedging. The water mixed with abrasive particles enters the gaps between fiber laminates, such as in 5c, and the cracks will increase further. This is how the delamination is happening due to abrasive particles [27]. In the case of AWJM, the major reason for delamination is the use of abrasive particles. At the same time, these particles are making the cutting process smoother in AWJM.

Fig. 10 shows the particles embedded between the fiber laminates. From the experiments, Shnmugam *et al.* [28] found that one of the major reasons behind this defect is the shock wave effect produced from the high-pressure AWJM. Some parameters, such as material thickness, orientation of fiber, and feed rate of the machine, also control delamination of materials [29].

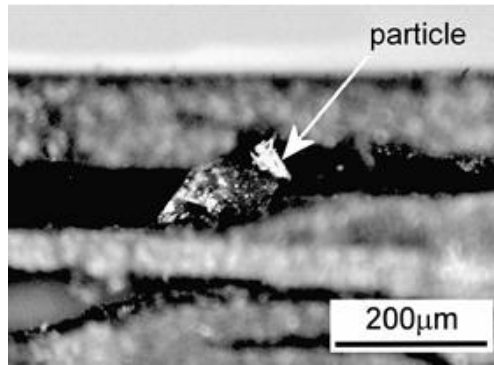


Fig. 10. Abrasive particles embedded between the laminates [27]

1.4. AWJ Cutting Quality

1.4.1. Geometric Variations on Cut Surfaces

There are three major types of phenomena observed during the cutting operation of composites, which are the presence of trail back, taper angles, and waviness on the surface. Sometimes, during cutting, the water jet deflects in the direct opposite side of the cutting action, resulting in a small exit lag behind the point of water jet entrance, which is known as the trail back shown in Fig. 11 [30].

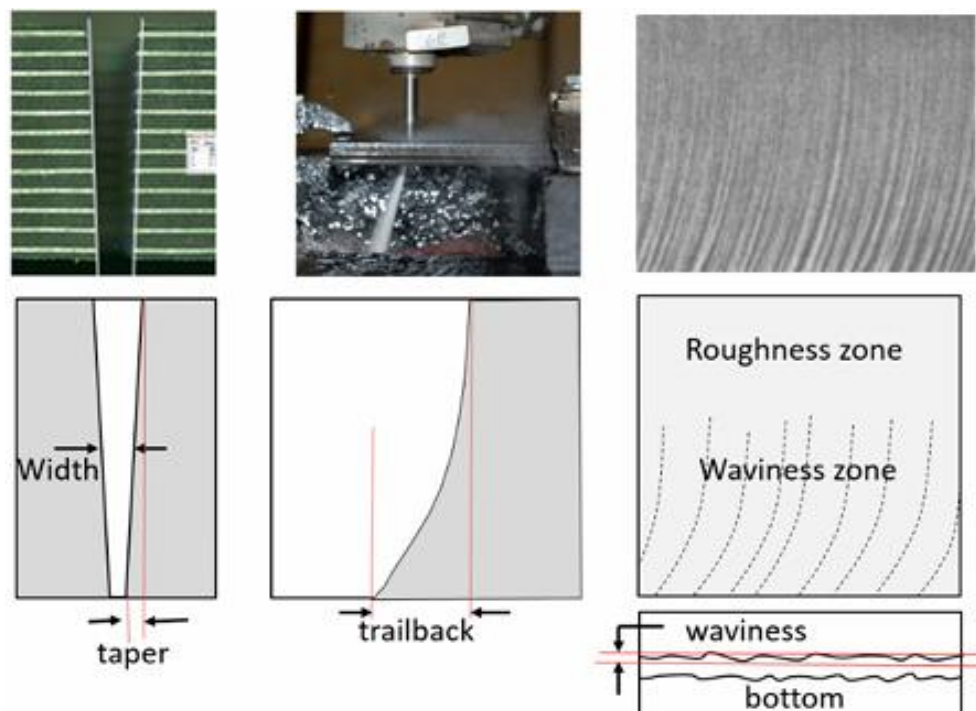


Fig. 11. Different phenomena observed on cut surfaces [30]

The next one is the difference between the cut width of the top and bottom surfaces of the samples. This difference is known as taper, and there will be the presence of an angle is called taper angle, used for checking the quality of cutting using AWJM. The presence of the taper of the cut is also shown in Fig. 11. The final one is normally related to the surface finish and called waviness on the surface. The reason behind this phenomenon is the striation happening due to the instability of the water jet at the end of the cut. This also shown in Fig. 11 [30].

1.4.2. Kerf Angle

Compared to other non-conventional methods, the AWJM does not produce heat-affected zones. There are many damages and defects that can occur to the workpiece during cutting operations performed using any cutting method. The reason for these defects can be different, from the feed rate to the stand-off distance of the beam [31]. Soft materials can be easily cut using a simple water jet mechanism in which these materials undergo ductile erosion. At the same time, AWJM is suitable for this kind of material. This erosion varies with the impact angle on the workpiece [32]. The kerf angle is an important parameter to assess the quality of cutting [32].

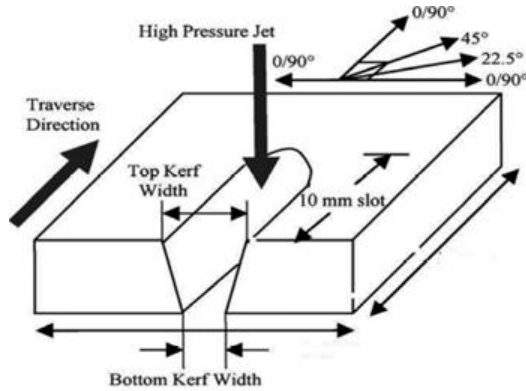


Fig. 12. Kerf plot geometry [34]

$$\tan \beta = \left(\frac{W_t - W_b}{2 \times t} \right), \quad (1)$$

where, W_t is the top kerf width (mm); W_b is the bottom kerf width (mm), and t is the thickness (mm).

The kerf and surface roughness values depend on some parameters called transverse speed and water pressure [32]. If the transverse speed and stand-of-distance (SOD) values are less, it will produce more vertical kerf walls. By increasing the jet speed and decreasing the transverse speed, SOD can result in low kerf angle values [33]. In addition, the kerf taper angle increases with fibre orientation in samples, where the 45° orientation gives a higher value for the delamination factor compared to the 60° and 90° (Fig. 12). The equation to calculate the kerf angle is Eq. 1 [33].

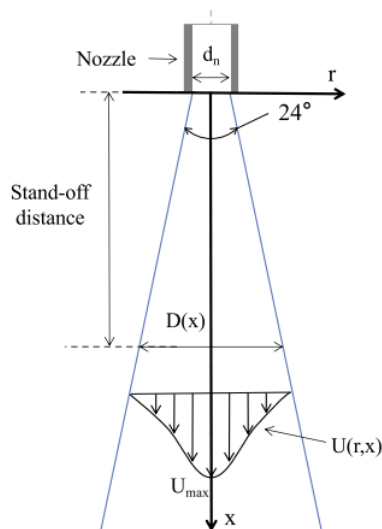


Fig. 13. Energy distribution of water jet from the nozzle to the material surface [36]

Eq. 1 can be used for calculating the taper angle values after the cutting operation using AWJM. The researchers studied the connection between the kerf characteristics and AWJM parameters by conducting numerous experiments. From the results, a certain transverse speed was found to depend on the nozzle size and workpiece thickness [35]. Some other researchers have tried another way to improve surface quality, like tilting the nozzle during the machining operation. Another method adopted is the inclination of the nozzle to analyze the relationship between the parameters and the nature of the kerf on the material [36]. Fig. 8 shows the energy distribution of the water jet from an AWJM during the cutting process. The kinetic energy is high at the center of the water jet. The velocity of the water jet is also very high at the central part of the water jet [36].

From the center to the far side of the water jet, the kinetic energy and concentration of abrasive particles will reduce [36]. During the cutting process, the abrasive particles help to get a better processing result for materials [36]. Even though the abrasive particles are not able to reach a velocity higher than the feed rate of water, this is due to the slip velocity [36]. Abrasive particles have large mass and sharp edges, which are helpful for the removal of material [36]. The energy of jet velocity is gradually lost with increasing depth of cutting, which is shown in Fig. 13.

1.4.3. Surface Roughness

Surface roughness values help to identify the characteristics of the surface of a material. This value can determine the quality of a surface and also determine its nature to other materials. It also helps to calculate the adhesion values of a material surface [37]. There are a few factors that affect the roughness of a cutting surface, such as the speed of the cutting source, the flow of abrasive material, the hardness of the sample materials, the SOD and the wear of the nozzle [38]. In case of AWJM SOD and abrasive flow are very important parameters to obtain very good cutting or machining quality. Fine cutting methods produce smooth surfaces because the transverse speed is slow, while the surface roughness is very high in the case of coarse cutting due to the high speed [38]. The main roughness values to consider to evaluate the quality of cutting are R_a and R_q values. R_a represents the arithmetic mean value, and R_q represents the root mean square value [39]. Fig. 14 shows the visual representation of R_a and R_q values in a graph.

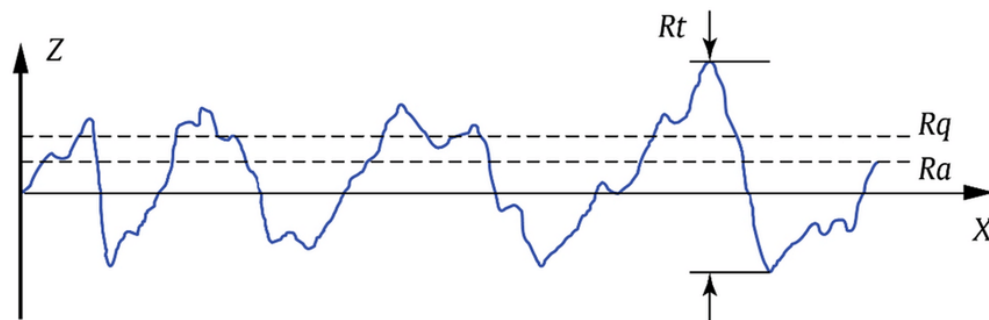


Fig. 14. R_a and R_q values [38]

R_a is the arithmetic average roughness of the deviations in absolute values of the surface height measured from the mean line over a given length [39]:

$$R_a = \frac{1}{L} \int_0^L |z(x)| dx; \quad (2)$$

Where L is the evaluation length; $z(x)$ is the surface height deviation from the mean line at the position

R_q is root mean squared roughness, mean of the squares of the surface height deviations [39]:

$$R_q = \sqrt{\frac{1}{L} \int_0^L z(x)^2 dx}; \quad (3)$$

Where L is the evaluation length; $z(x)$ is the surface height deviation from the mean line at the position

Equation 2 can be used to calculate the R_a values, and Equation 3 can be used to calculate the R_q values. R_q values are more sensitive to variations on the surface than R_a values. Therefore, R_q values are considered for a more accurate study of surfaces. The cut quality of a material can be predicted by studying the roughness characteristics of a surface [39]. From the GFRP experiment conducted, the researchers found that the surface roughness varies with the pressure of the water jet [40,41]. The orientation of the fibres also has an important role in determining the level of surface roughness. In case of CFRPC, the orientation shows a very good result compared to the 60/90 orientation [41].

1.5. Texturing of Composites

Texturing the surfaces of composites is a technique of modification for surfaces for various purposes. Texturing can be used to repair materials or even for improving the performance of the materials. The quality of the texturing, such as type and size, can be varied with the texturing methods employed [42]. Laser surface texturing is a common method for the micro-texturing of polymer materials. Two types of results can be obtained on polymers using laser beam texturing, such as dimples or grooves, as shown in Fig. 15. Fig. 16 shows the schematic diagram of the laser texturing method used for polymer texturing. In this method, the laser beam is pointed at a point with the help of a lens, and the texturing patterns are produced [43].



Fig. 15. Laser texturing results (a) dimples and (b) grooves [43]

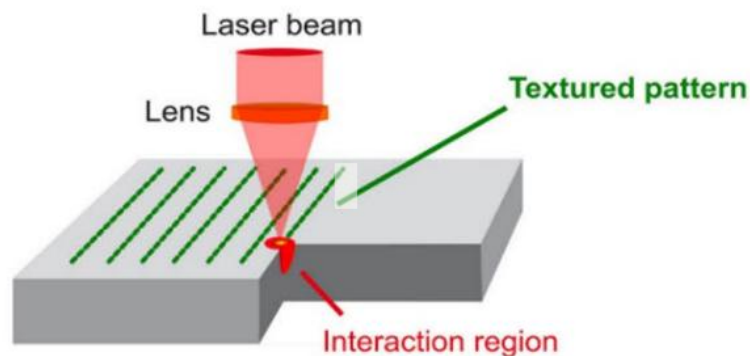


Fig. 16. Schematic for micro-texturing of polymer using the laser beam [43]

Laser surface texturing is a non-contact process, and, compared with other surface modification techniques, LST has numerous advantages. High quality, minimal waste, and less processing time are some of those advantages [44]. One of the other methods for micro-texturing of polymer materials is electrochemical machining, which is shown in Fig. 17. Basically, it is the easiest method and is mostly used for conductible materials because the material is removed through the anodic dissolution. Even though a modern version of this method can be used for machining polymers and it is called electrochemical-electrodischarge machining [45].

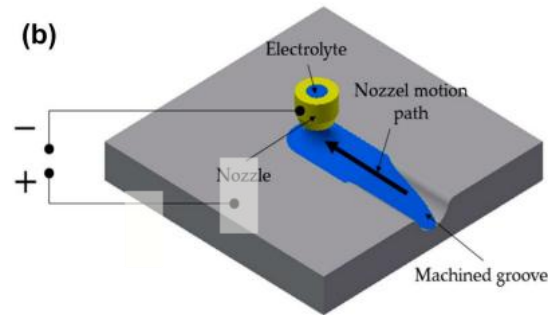


Fig. 17. Electrochemical machining [45]

The texturing of composites is used for different purposes, one of which is the repair application of materials [46]. CFRPC use is very common in aerospace engineering these days for multiple reasons, such as better strength-to-weight ratio, corrosion resistance, and thermal insulation [46]. Maintenance of CFRPC composite structures sometimes requires removal of materials. The material removal can be achieved by different methods, such as machining or texturing. The repairing of CFRPC requires material removal from the damaged section. During machining, the material removal rate is much higher compared to the texturing, allowing the operator to control the modification on the material and enhance the adhesion [46]. Normally, the texturing and machining of materials is done by traditional methods in industries [47]. material removal results in numerous defects and challenges [48]. Complications of the process are one of the major challenges related to this process when using old methods. Delamination and fiber pull-out are the normal defects associated with the conventional methods. Therefore, the texturing of composites is not very easy to achieve using conventional methods [48].

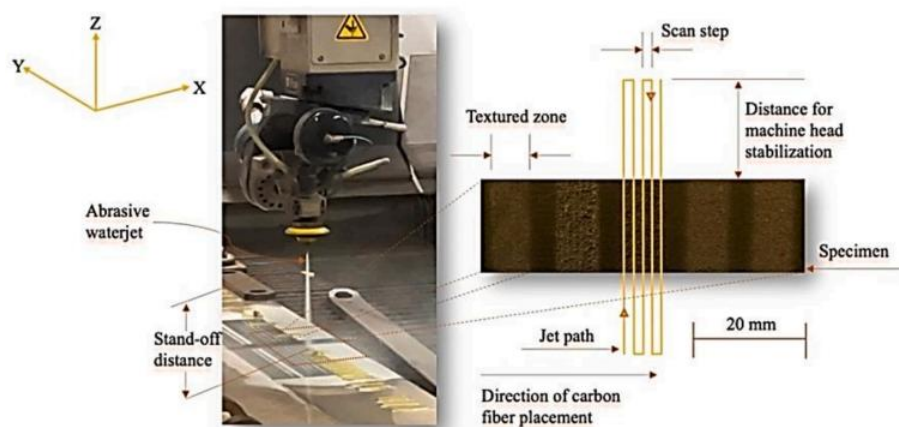


Fig. 18.AWJM is used for repairing the CFRP in the aerospace industry [46]

Due to these challenges and defects associated with the normal method, industries are exploring the modern method available in the market to achieve great results [49,50]. Although the modern method also faces challenges with the machining and texturing of composites. Laser beam machining of CFRP shows the result of delamination, heat formation, and cracks in the matrix [51]. The electric discharge method also exhibited some defects, such as delamination, thermal degradation, and swelling of the fiber. Among these methods, the modern AWJM method shows more potential for both texturing and machining composites [52]. Using AWJM for material removal does not produce any issues with heat generation [53]. During the operation using AWJM, the input parameters like the pressure of the water jet, the feeding rate, and the stand-off distance are more important to obtain good surface quality and results. The given Fig. 18 shows an example for an AWJM used for repairing the CFRP in the aerospace industry.

1.6. Chapter Summary

AWJM is a very suitable method for cutting composites in comparison to many other methods currently available in the modern market. There are many reasons for this, like this method does not create an affected zone after cutting and is more cost-effective. Moreover, the ease of handling the machine is another reason to use AWJM as a machining option for composites. but machining using AWJM produces some defects like delamination of fiber laminates, fiber pull-outs in the machined parts. The reason for these defects also varies with different parameters. The cutting of composite material using this method is associated with numerous other factors to evaluate the quality of the cutting. Kerf angle values and surface roughness analysis are options to investigate and evaluate the cutting results of AWJM. The possibility and importance of texturing using AWJM are also investigated. By studying the possibility of AWJM for texturing shows that it reduces defects during the texturing operation, which occur from the traditional methods, such as heat production.

2. Materials and Experimentation

2.1. Materials

Twill weave glass (160 g/m²), carbon (160 g/m²), aramid (170 g/m²), and basalt (220 g/m²) fibers were used for the preparation of composite laminates. Epoxy resin L and a hardener S (R&G Faserverbundwerkstoffe GmbH, Epoxy Resin L, Hardener S). It is a two-part system where the epoxy is the base resin and the hardener is the curing agent.

Materials used for vacuum bagging were: GREY vacuum sealing tape with a dimension of 3 x 12 mm x 5 m, the nonwoven absorber layer Breatex TM with a surface density of 150 g/m², and a perforated plastic film. The bagging film used is 50 µm in thickness and 125 °C of temperature resistance, with a width of 145 cm. The plain weave peel ply (64 g/m²), and a transparent vacuum tubing with a diameter of 6/8 d 10/12 mm were used.

2.2. Preparation of Composite Laminates

In this experiment, four types of composite laminates were used to cut and evaluate the quality of AWJM cutting through different analyses. The composites were obtained using a hand-layup technique with the support of the vacuum-bagging technique. The four fibers used have an orientation of 0/90°. All composite laminates have 60% reinforcements and have a thickness range of 2-3 mm. Resin is mixed with the hardener in a 7 : 3 ratio. For the composite preparation, the fibers were cut into 10 different pieces with a dimension of 100×100 mm. Then, an open mold is prepared with bagging film, peel ply, and non-woven absorber. All fiber pieces are put one on top of another, and each time, the mix of resin and hardener is applied between these layers. After finishing 10 layers, the mold was sealed with sealing and went through a vacuum bagging section using a vacuum machine. After all of these processes, the vacuum bag with samples was left to cure at room temperature. Fig. 19 shows the prepared samples of GFRPC, CFRPC, and BFRPC.



Fig. 19. Vacuum bagging

2.3. Cutting of Samples Using AWJM

After the preparation of the composites, the next step was cutting these samples with the help of an AWJM machine to evaluate the cutting quality. The cutting machine used for the experiment is the *Wazer desktop* AWJM, shown in Fig. 21, which is manufactured by the company named *Wazer*. The technology used to cut the samples using this machine is the application of a high-pressure water jet with a mix of abrasive particles. This machine has an online platform called WAM, where we can input the cutting shapes and adjust the transverse speed and a few other parameters. The abrasive particles used in the cutting process were 80 mesh alluvial garnet, which is very popular in the market due to its quality. A high-pressure water jet with a mix of 80 mesh alluvial garnet was used to cut the samples in a square shape with 30×30 mm dimensions. The cutting and electrical parameters of the *Wazer Desktop* are given in Table 2. Fig. 20 shows the cutting path used for cutting the composite samples in a square shape. This cutting path is generated with the help of solid SolidWorks software. Before cutting the samples, the cutting path was converted into the required format for Wazer AWJM using the online platform of the Wazer company. The starting and ending points of the cutting were the same, and the water jet always stayed at the starting point for a few seconds before starting the cutting process. For cutting the sample, the cutting path file was loaded into the machine with the help of a digital memory card. After selecting the required cutting file and following the cutting instructions of machine, the cutting operation was done.

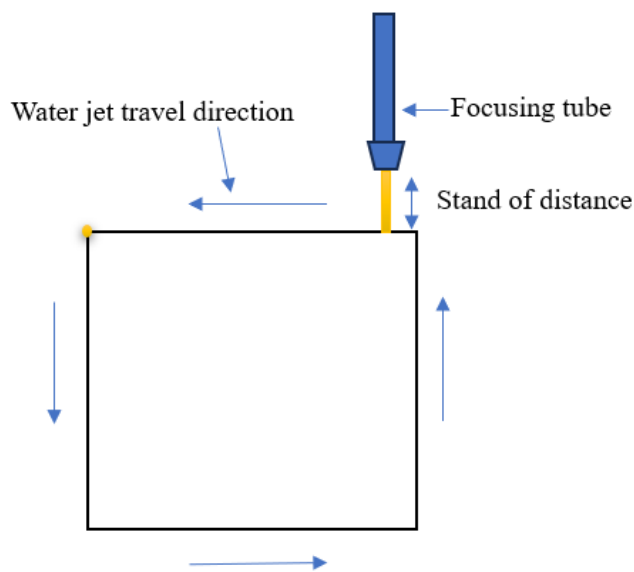


Fig. 20. Cutting direction of samples

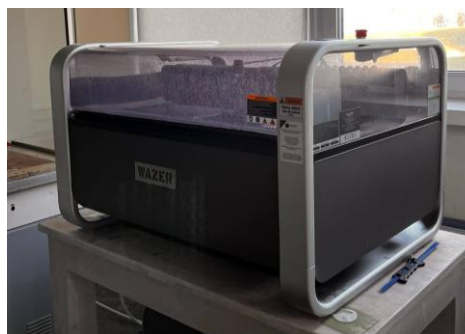


Fig. 21. *Wazer Desktop* AWJM

Table 2. Cutting and electrical parameters of *Wazer Desktop AWJM*

Parameters	Values
Cutting Area (D x W)	305 × 460 mm
Working pressure	275 bar
Cut Bed Size (D x W)	330 × 485 mm
Kerf (width of cut)	1.1 mm
Abrasive Rate	0.15 kg/min
Power Requirement	220V / 50Hz (International)
Cutting Speed	Variates by material and thickness.
Hydraulic power	820 W
Orifice Diameter	0.48 mm
Abrasive Hopper Capacity	13.5 kg
Abrasive Rate	0.15 kg/min
Continuous Cutting Time	60 min

2.4. Surface Roughness Analysis Using ImageJ Software

Following the cutting action, all samples were examined with an optical microscope called ECLIPSE LV100ND_Nikon to evaluate the nature of the surface of each sample. Surface pictures of every sample were taken to examine these pictures in a surface roughness value calculating software called ImageJ. ImageJ is a software used for microscopic image analysis and surface roughness analysis. Using ImageJ software, profilograms of each cutting sample were taken and evaluated. Profilograms are the graphs of a machined or cut surface that commonly focus on the height variation on the surface. Surface roughness analysis is a method used to find the roughness and smoothness of a surface by evaluating the texturing of a machined surface. The main parameters of this analysis are R_a and R_q . These cut samples were calculated using ImageJ software. Fig. 22 shows the optical microscope used to take images of composite materials.



Fig. 22. Optical microscope ECLIPSE LV100ND_Nikon

2.5. Kerf Angle Measurement

After cutting the samples using *Wazer Desktop* AWJM, these samples were used for measuring the kerf angles of cuts. Kerf angles were measured using the optical microscope ‘Moticam 1000 1.3M Pixel’ and ‘Motic Images plus 2.0’ software. Kerf angles were calculated from four measurements. Using the same microscope, a qualitative study of the delamination images was carried out to investigate the presence of delamination after the cutting process.

2.6. Texturing on Composites

Following the cutting process of composites, another study was performed on the samples to analyze the effect of texturing on the composites. The same samples with the same dimension were taken to finish this process. All composite samples were placed on the same *Wazer desktop* cutting machine to check the texturing effect. This experiment was carried out by varying two major parameters of the cutting machine, one of which is the stand-off distance and the other is the transverse speed. The standoff distance of the machine can be easily varied by moving the tip of the water jet pumping tool. The transverse speed of the machine can be varied inside the programme file exported from the online platform of the *Wazer Desktop* machine, where the cutting tool path is imported and creates the cutting file for individual samples. Speed was changed in the Notepad software available on Windows. Using this method, we can attain any variation in the speed, such as an increase or decrease in values. Four standoff distance (SOD) values were taken into account to check the changes in the texturing process, which are 2.28 mm, 4.56 mm, 6.84 mm, and 9.12 mm. At the same time, five traverse speeds were used to analyze the variation in texturing effect, which are 70 mm/s, 100 mm/s, 150 mm/s, 200 mm/s, and 250 mm/s.

During the experimental section as a first stage, the variation of SOD was examined on AFRPC with normal coarse transverse speed, which is 70 mm/s. In all SOD values the AFRPC sample does not exhibit any evidence of texturing and all those ended up as cutting. So from the next step the closest SOD value was chosen as a constant, and the transverse speed varied increasingly from 70 mm/s to 250 mm/s. Following this process in the next stage the highest value transverse speed was maintained as a constant value and the SOD varied from 2.28 to 9.12 mm. After these processes two more cuts were done on samples with the transverse speed of 300 mm/s and 350 mm/s by keeping the SOD constant at 2.28 mm. Not only AFRPC but also CFRPC, GFRPC, and CFRPC went through the same process to find the effect of texturing on these composites using the *Wazer desktop* AWJM. After this process, all samples were examined using an ECLIPSE LV100ND_Nikon, to examine the quality of texturing by measuring the kerf width values of the top and bottom of the cuts. These values were used to compare the quality of the texturing in the composite samples.

2.7. Chapter Summary

The composite materials were prepared using the hand layup process, then the composite samples were cut with two feed rates using a *Wazer Desktop* AWJM in a small square shape with a dimension of 30 × 30mm. After the cutting process, the cut specimens were examined using an optical microscope to take pictures for further processing. The kerf angles of the samples were measured using the Moticam 1000 1.3M Pixel. The texturing effect on the samples was also analyzed using the same AWJM and microscope.

3. Comparison of Processing Reactions of Basalt Fibre-Reinforced Composites with Aramid, Glass, and Carbon Fibre-Reinforced Composites

3.1. Quality of Cut Samples

In order to compare the reactions of the basalt fibre machining process with aramid, glass, and carbon fibre reinforced composites, composite specimens with the same number of plies were cut using the same cutting parameters. It should be noted that the thicknesses of the composite laminate samples varied slightly depending on the type of fibre used for the reinforcement. Two feed rates were selected as offered by the software of the machine: fine cutting at a feed rate of 50 mm/s and coarse cutting at a feed rate of 70 mm/s. The SOD was always constant at 2.28 mm during the cutting process. The results of the specimens cut under both cutting conditions are shown in Table 3. Studies have shown that the nature of the reinforcing fibre has a significant influence on the cutting process and the final cutting quality. It is clearly evident that every sample has a good quality of cuts and the major problem faced was delamination.

The optical microscope images of the cross-sectional surface shown in Table 4 make it easier to identify the individual layers of the laminate and the interactions between them. The presence of delamination is evident in almost every sample except CFRPC. For BFRPC, AFRPC, and GFRPC samples, the delamination is clearly visible at the corners where the cut begins. Delamination is a common defect that occurs during the composites cutting process [36]. It can be seen that the delamination occurred at the edge from which the cutting process started. The investigations of Shanmugam et al. [36] show that the delamination is caused by a shock wave caused by a water jet and the abrasive particles used in the cutting process. Not only that, but also the bad adhesion of the matrix and reinforcement can also create such delamination defects during the cutting process.

BFRPC is one of the latest materials used among the four fibers, which shows evidence of delamination. The reasons behind the delamination on BFRPC are the shock wave caused by the water jet machine. One more reason that can be included in the list of BFRPC delamination is the poor adhesion of the matrix and reinforcement can also create such delamination defects during the cutting process. This was clearly visible in the BFRPC result, and the main delamination point was the cutting corner where the process started and ended. When the CFRPC samples with BFRPC, it has the highest cutting quality among all samples because they do not exhibit any evidence of delamination or any other kind of defects. In addition, the cutting edges were very smooth and the layers of carbon were well bonded to the resin. This is understood by comparing this with BFRPC cut samples, where the cutting process starts and ends, with the presence of delamination evident at the edges. CFRPC showed good quality and surface finish on both types of cutting with different feed rates compared to BFRPC. AFRPC cut samples comparison with BFRPC shows the result for both fine and coarse cutting, that very good cutting quality and finish of surface obtained on AFRPC cut samples, but the presence of delamination on corners where the cutting started was visible. In AFRPC, the main reason for this delamination was the same as in BFRPC, the sock waves of the water jet, and one more thing to consider is that the AWJM nozzle usually stays at the same point for a short period of time, which also caused another reason behind delamination in AFRPC. GFRPC also exhibited the presence of delamination on the same corner as BFRPC, the reason is also the same as that of AFRPC and BFRPC. GFRPC also exhibited good quality of cut and surface finish when compared with the results of BFRPC. The presence of fiber pull-out defects was also visible, mainly in BFRPC and AFRPC cut samples.

Table 3. Images of cut samples of composites for coarse and fine cutting

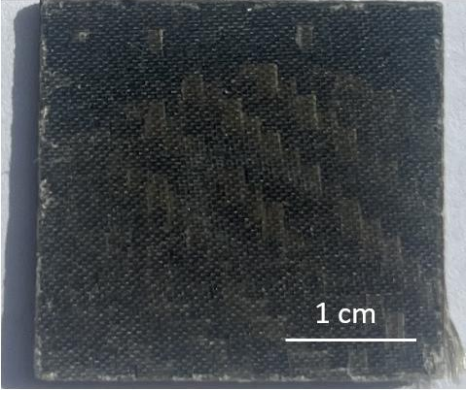
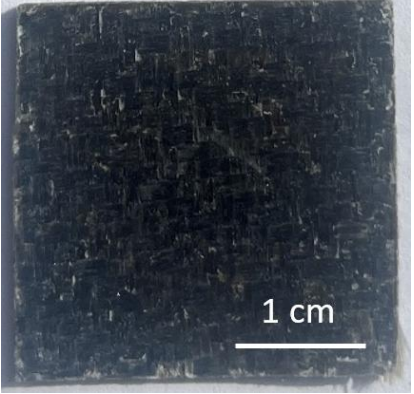
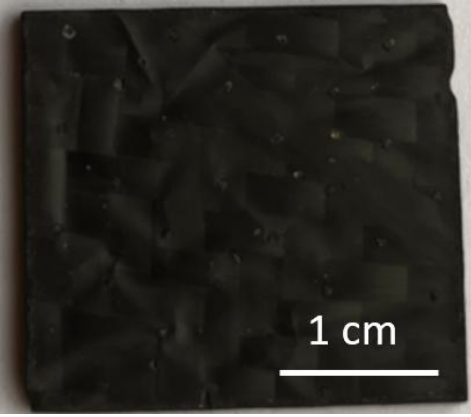
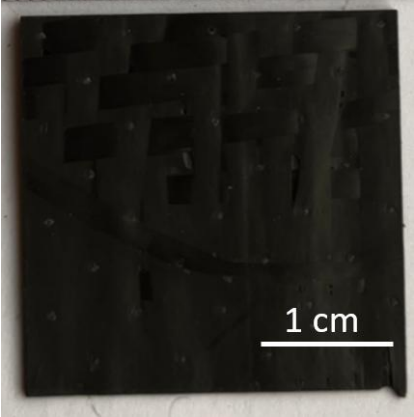
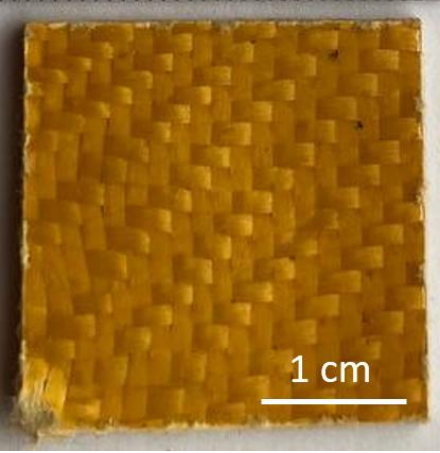
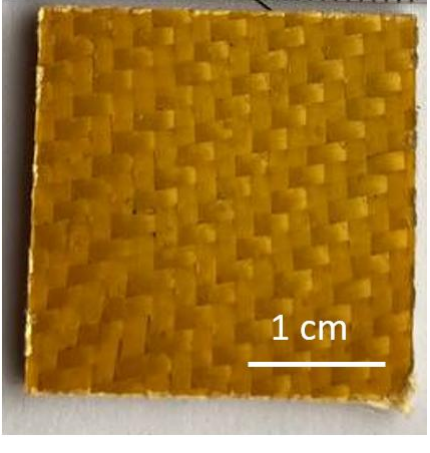
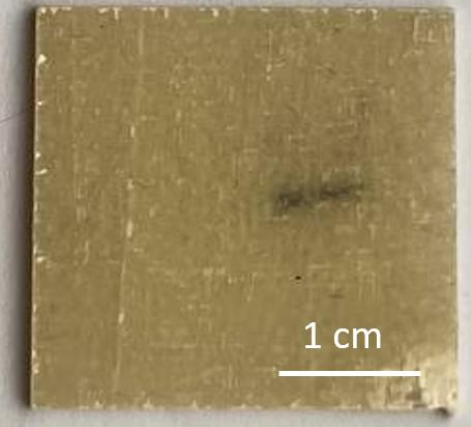
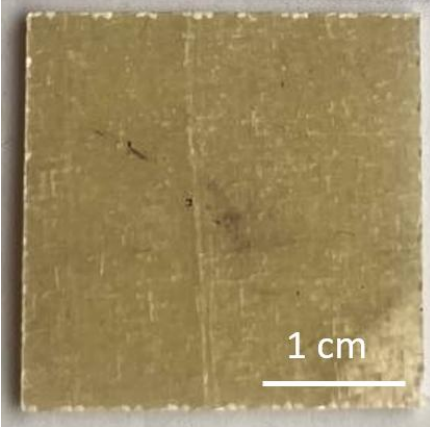
Composite material	Coarse cutting (70mm/s)	Fine cutting(50mm/s)
BFRPC		
CFRPC		
AFRPC		
GFRPC		

Table 4. Delamination on BFRPC, AFRPC, and GFRPC samples, coarse cutting (e) and fine cutting (f)

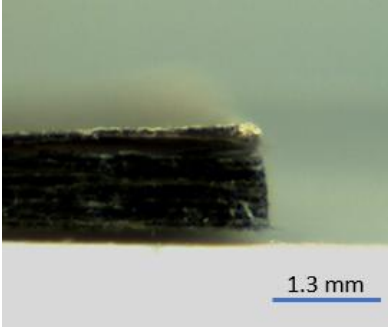
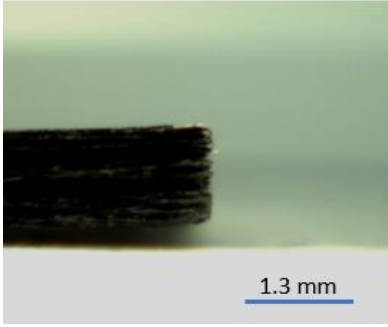
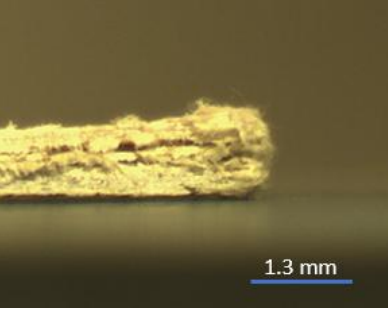
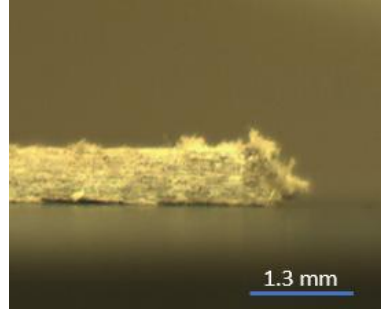
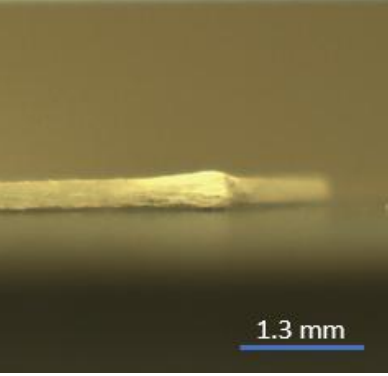
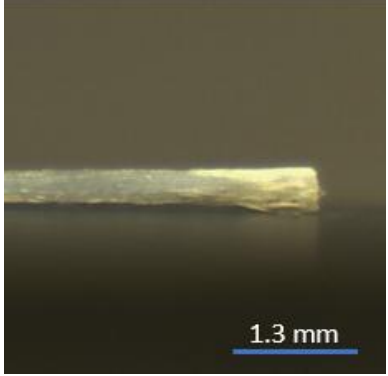
Composite material	Coarse cutting	Fine cutting
BFRPC		
AFRPC		
GFRPC		
	e	f

Table 4 lists the optical microscopic images of delamination evidence of BFRPC, AFRPC, and GFRPC samples. These are the three FRPC exhibited delamination defects at the corners. Table 5 shows the optical microscopic images of FRPC cross sections for coarse and fine cutting with a scale of 500 μ m. These photos clearly show the presence of major defects in these four FRPCs. The optical microscopic images of BFRPC cross sections clearly show the fiber pullout defects in both fine and coarse cuttings. The high amount of fiber pullout is visible in BFRPC compared to all other composite cross sections. Compared to the result of BFRPC with the optical microscopic image of CRFPC, it shows very good results of cross-section with zero evidence of defects like delamination, fiber pullout, and any kind of tearing inside the sample. AFRPC cross sections show very good results with very little evidence of defects compared to BFRPC. The presence of fiber pull-out is visible in AFRPC, but it was rare in limited spots. In over all the number of defects is less in AFRPC when compared with the images of BFRPC. FRPC images show something more than the results of BFRPC, that the presence of a small crack inside the fine cutting sample. Compared to BFRPC, the presence of fiber pullout and delamination was less in GFRPC. Still, the defects were visible on a very small scale in GFRPC samples. Overall, all only the CFRPC exhibited an excellent result compared with BFRPC.

Table 5. Optical microscope images of composite cross-sections of coarse and fine cutting

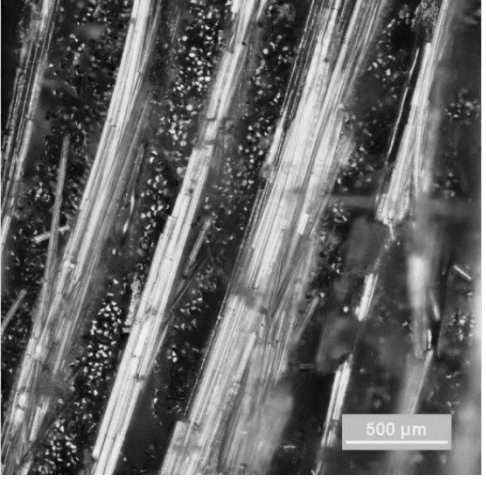
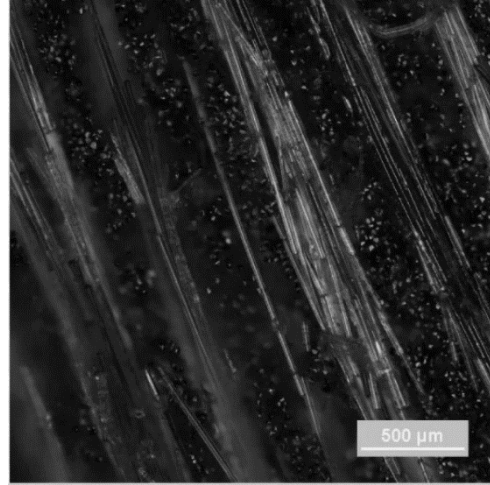
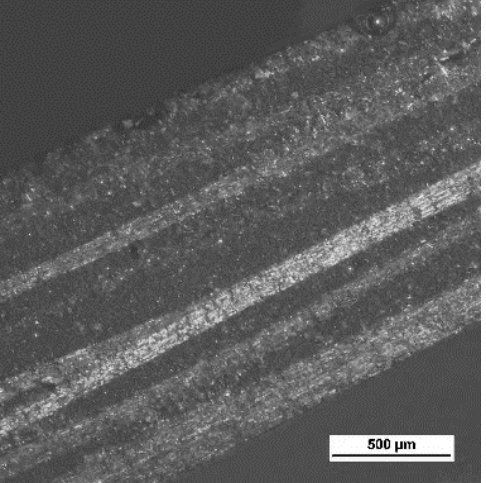
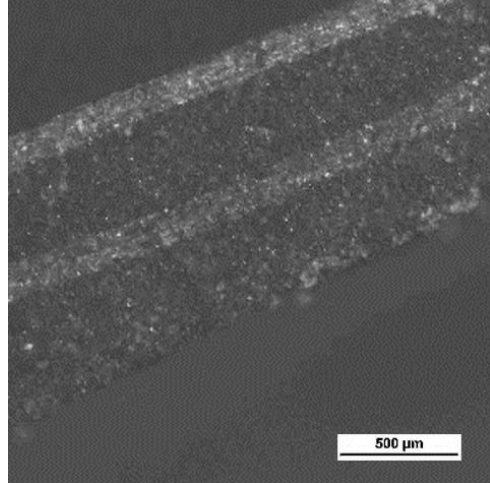
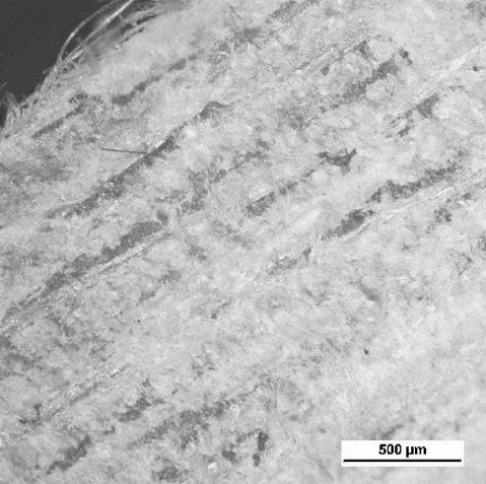
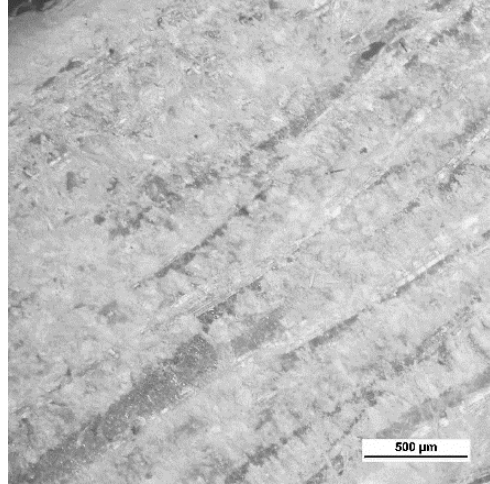
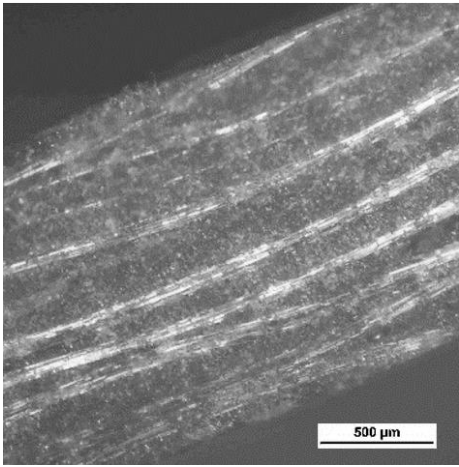
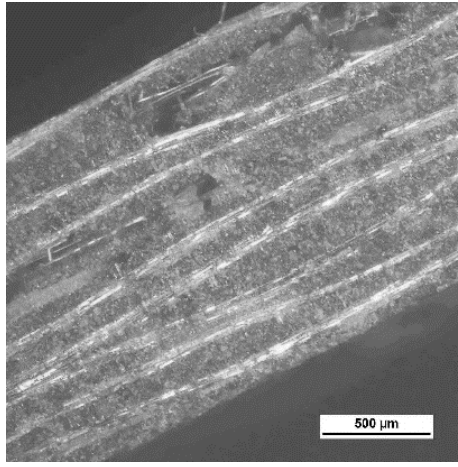
Composite material	Coarse cutting (70mm/s)	Fine cutting(50mm/s)
BFRPC		
CFRPC		
AFRPCC		

Table 5. Optical microscope images of composite cross-sections of coarse and fine cutting

Composite material	Coarse cutting (70mm/s)	Fine cutting(50mm/s)
GFRPC		

3.2. Surface Roughness Analysis

The profilograms used for calculating the surface roughness values of FRPC obtained using ImageJ software are shown in Figures 23, 24, 25, and 26. All these profiles are measured from a picture of samples with 32 bits. In profilograms, the X-axis represents the scan length across the FRC, and the Y-axis represents the brightness of each pixel in the image. The higher peaks in the profile indicate the brighter areas in the scanned picture, and the lower peaks represent the darker areas. In this profile, the grey scale value varies differently based on the quality of cutting. These graphs are used to identify surface irregularities by measuring fluctuations. These higher and lower peaks can indicate the delamination, irregular cutting, and debonding of fiber from the composite. After creating these profilograms, the Surfchar J plugin from ImageJ software was used to get the surface roughness values of the FRPCs.

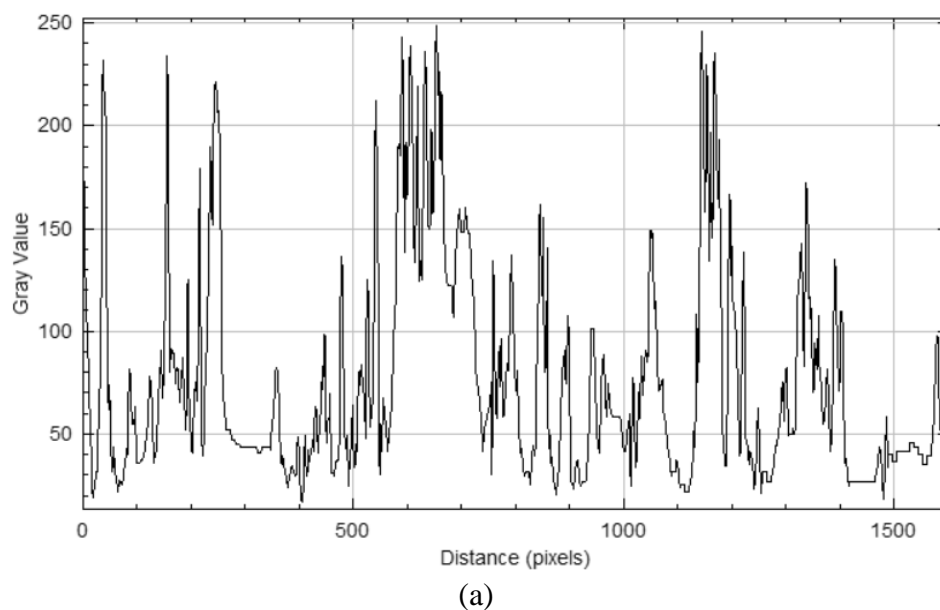


Fig. 23. The profilogram of the BFRPC surface after cutting (a) coarse, (b) fine

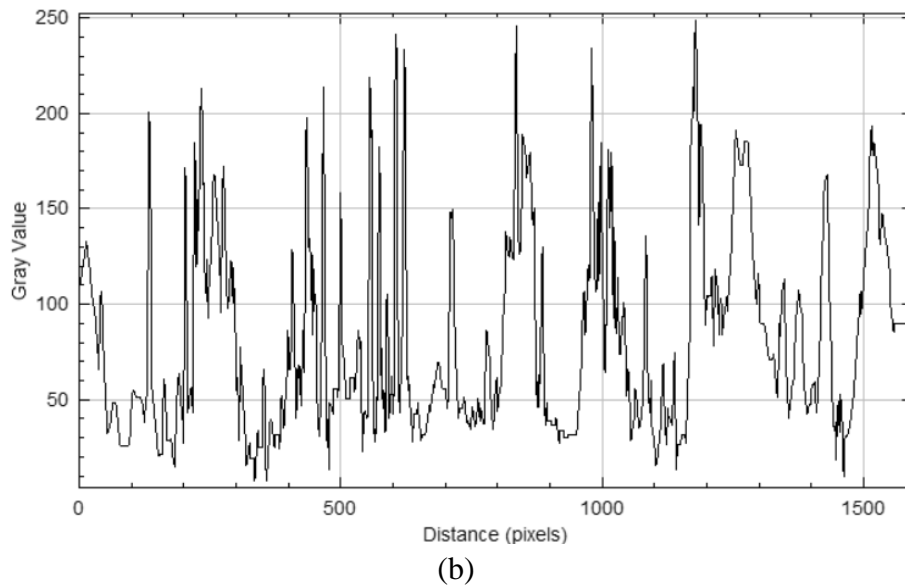


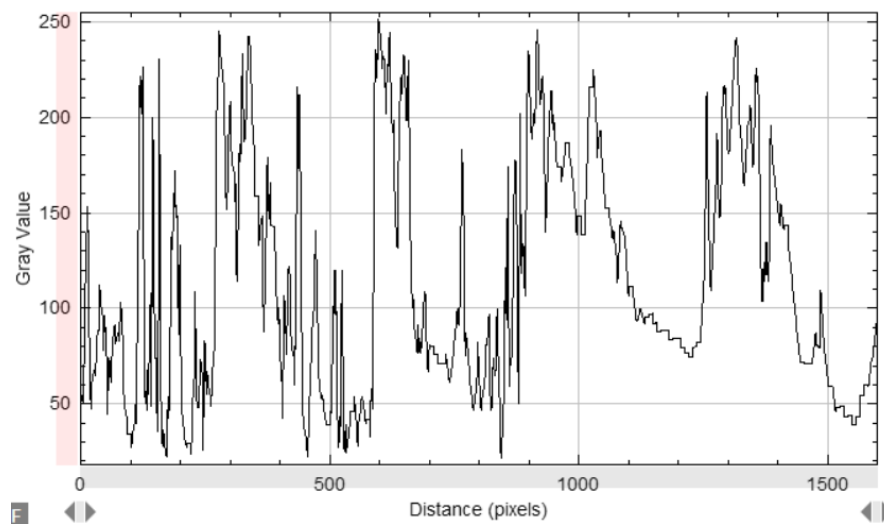
Fig. 24. The profilogram of the BFRPC surface after cutting (a) coarse, (b) fine

Figs. 23a and 23b are the profilograms of coarse and fine cutting specimens, respectively. From these profiles, the x-axis represents the grey value and the y-axis represents the distance in pixels. Here, coarse cutting profiles exhibit a high profile variation, which indicates the rough surface. In coarse cutting profile, the grey scale value ranges from 0 to 250. The highest value achieved is also close to 250. Moreover, the grey scale value variations along with the distance are not uniform; the presence of wide gaps between the peaks and valleys is clearly evident. There is a wide gap between the distances 500 pixels to 1000 pixels, which is one of the clear evidences of surface irregularity in coarse cutting of BFRPC samples. The BFRPC fine cutting profile also has irregularities and a high variation in the grey scale value. In this profile, the grey scale values vary from 0 to 250. The highest value in this profile is near 250, but the variation in values is in more order compared to the coarse cutting profile. Higher variations in grey-scale values over distance represent bad cutting quality or a rough surface. For fine-cutting profiles, the peaks and valleys are more uniform and regular compared to the coarse-cutting profile. From the graphical representation of BFRPC samples, the rougher the surface obtained is from coarse cutting. The roughness values calculated from these graphs also support the same conclusions. The main reasons for high peaks and values in the coarse cutting profile can be defects such as delamination and fiber pullouts. The R_a and R_q values for both cuttings are found and listed in Table 6.

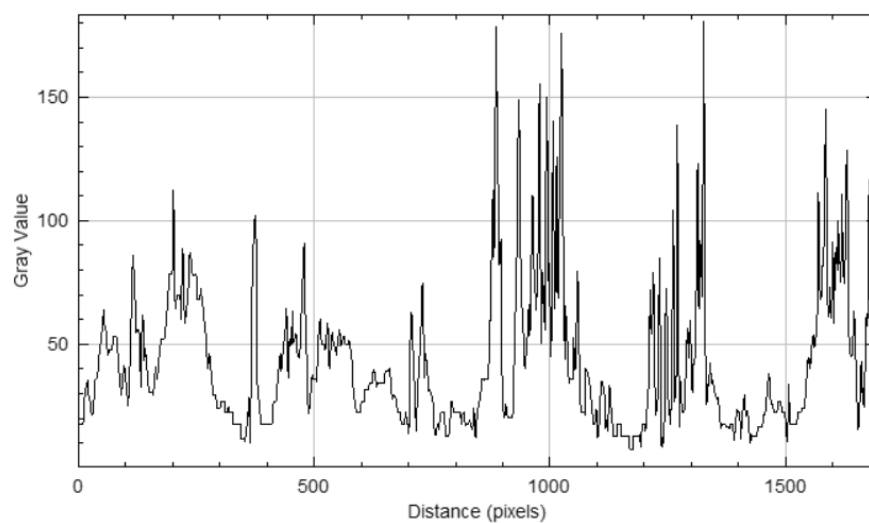
Figs. 24a and 24b are the profilograms of the coarse and fine cutting specimens, respectively. When comparing these graphs with BFRPC graphs, the coarse cutting profiles show a high variation in the graph, which indicates a rough surface. The same trend was shown in the BFRPC samples. From the profile, it is clear that the surface has multiple irregularities and high changes in the grey value. The variation in grey value is the same as that in BFRPC, where the highest value obtained is 250, and the values range from 0 to 250. The distance between the peaks and values was also higher, as in the coarse profile. The long gap between 1000 to 1500 pixels exhibits the presence of an irregular surface. Moreover, like the BFRPC coarse cutting profile, the high peaks and valleys stand for a surface that is not uniform. The fine-cutting profile shows different characteristics from the coarse-cutting profile, but it shows the same pattern as the BFRPC fine-cutting graph. The peaks and valleys present in the AFRPC fine cutting profile are more uniformly distributed than coarse-cutting. Something different from the BFRPC fine profile is that the highest value obtained here is just above 150, which is 100

values less than BFRPC. From these value differences, it is clear that the surface is smoother and more uniform than coarse cutting. The presence of higher value changes is also rare in this profile compared to the same profile of BFRPC. The major reasons for the high peaks and values in the coarse cutting profile may be the effect of defects such as delamination and fiber pullouts. From these profiles, the R_a and R_q values for both cuttings are found and are listed in Table 6. From these values and the graph, it is clear that fine cutting is better for BFRPC than coarse cutting because fine cutting is slower than coarse, even though it gives better smoother and higher quality without more complicated irregularities.

The noticeable change in AFRPC samples was the R_a and R_q values, which was very low compared to the surface roughness values of the BFRPC samples listed in Table 6. In the fine cutting profile of AFRPC, the variation of values between the distance from 0 pixels to almost 1000 pixels was very small compared to the coarse cutting profile of AFRPC and both profiles of BFRPC. This indicates the uniformity of the surface throughout that distance and the quality of cut was also very high at that point. Furthermore, there is an almost 10-point difference in the R_a and R_q values of AFRPC compared to the values of BFRPC. In simple words, AFRPC cut surfaces are better than BFRPC samples.



(a)



(b)

Fig. 25. The profilogram of the AFRPC surface after cutting (a) coarse, (b) fine

Figs. 25a and 25b are the profilograms of CFRPC coarse and fine cutting specimens, respectively. Compared to other composites, CFRPC shows good results in both profiles and numerical value of roughness for both cuttings. In the coarse cutting profile of CFRPC, the variations are lesser than compared to the same profile of BFRPC. The variation of grey value only ranges from 0 to a few points above 150. This is a huge difference from the coarse profile of BFRPC. This small variation in values indicates a less irregular surface. The good quality of the cutting in the CFRPC samples was very clear from the normal examination of both samples from the beginning. The CFRPC fine cutting profile shows more quality results and values than the BFRPC fine profile of BFRPC. In this profile, the highest value is only just above 140. This means the higher surface finish of the CFRPC sample compared to that of the BFRPC. Like the same in BFRPC, the CFRPC profiles of both cutting shows variations in grey values, but it was not too much compared to the BFRPC samples profiles, which show a good cutting quality. From the roughness values, fine cutting also gives better quality than coarse cutting for CFRPC. There is a very high difference in the numerical values of the the R_a and R_q values of CFRPC samples with the BFRPC values. It also indicates that CFRPC samples have a higher surface finish than BFRPC samples.

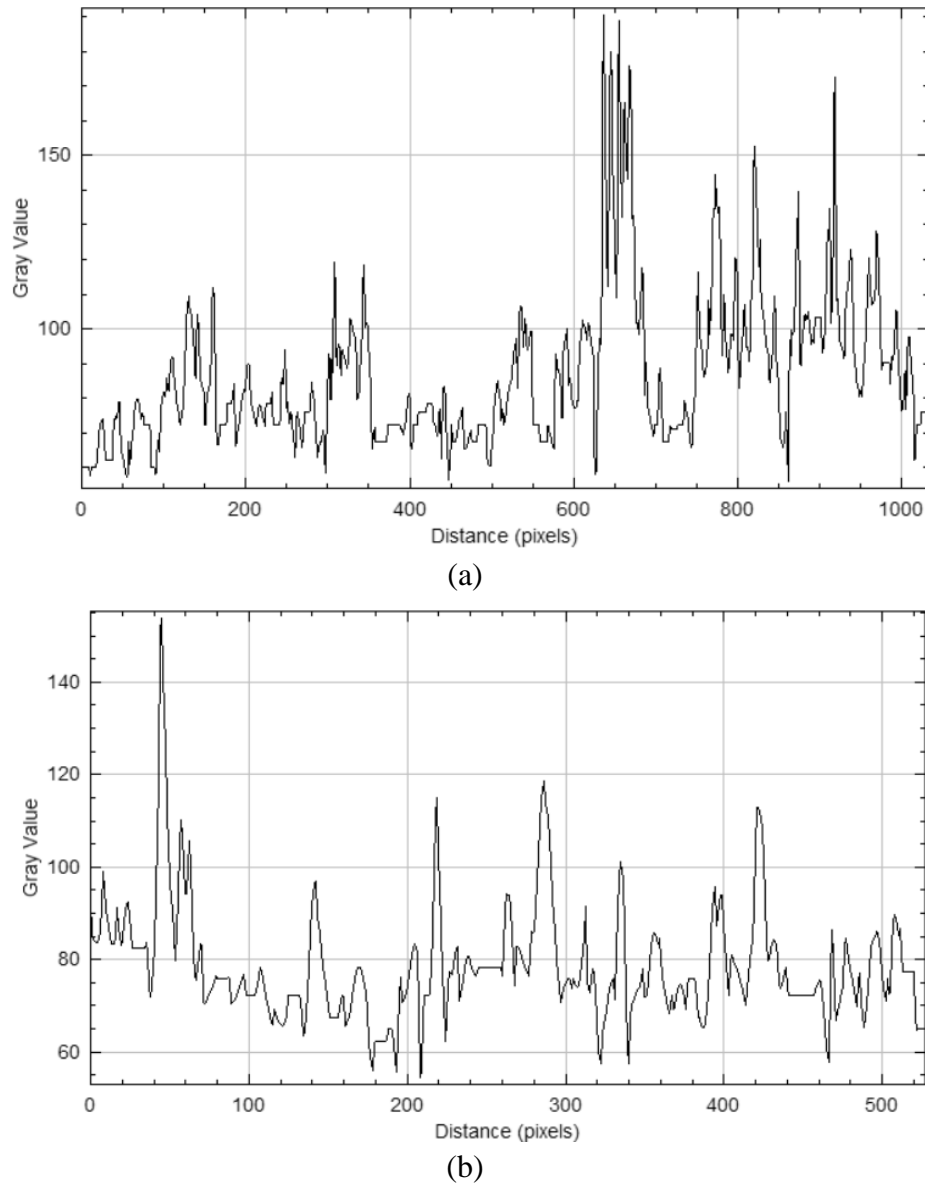


Fig. 26. The profilogram of the CFRPC surface after cutting (a) coarse, (b) fine

Comparing the values in the BFRPC profiles with Figs. 26a and 26b, the profilograms of the coarse and fine cutting specimens, the results are also different from those of other composites. Coarse cutting profile of GFRPC shows, with high peaks and valleys, which represent the rough surface. But in the GFRPC coarse cutting profile, the higher variation points of grey scale values are fewer compared to BFRPC. The highest value is similar to the highest coarse cutting value of BFRPC, which is 250. The higher variation in the surface was evident only in the distance between 400 and 800 pixels. At a distance between 0 to 200 pixels, the surface shows good results and less irregularity. When comparing the fine-cutting profile of GFRPC with the same profile of BFRPC, the variation in values is different. The highest variation in the measured grey scale value is just above 200, which is less than the highest value of the BFRPC fine sample. The fine cutting profile of GFRPC shows a lot of variation in values, but those variations are more uniform compared to that of BFRPC. The defects can be delamination, fiber pullouts, etc, which caused these variations in values. The roughness values of GFRPC are also less than the values of BFRPC this indicates that GFRPC has better quality in cut profiles compared to the cut samples of BFRPC,

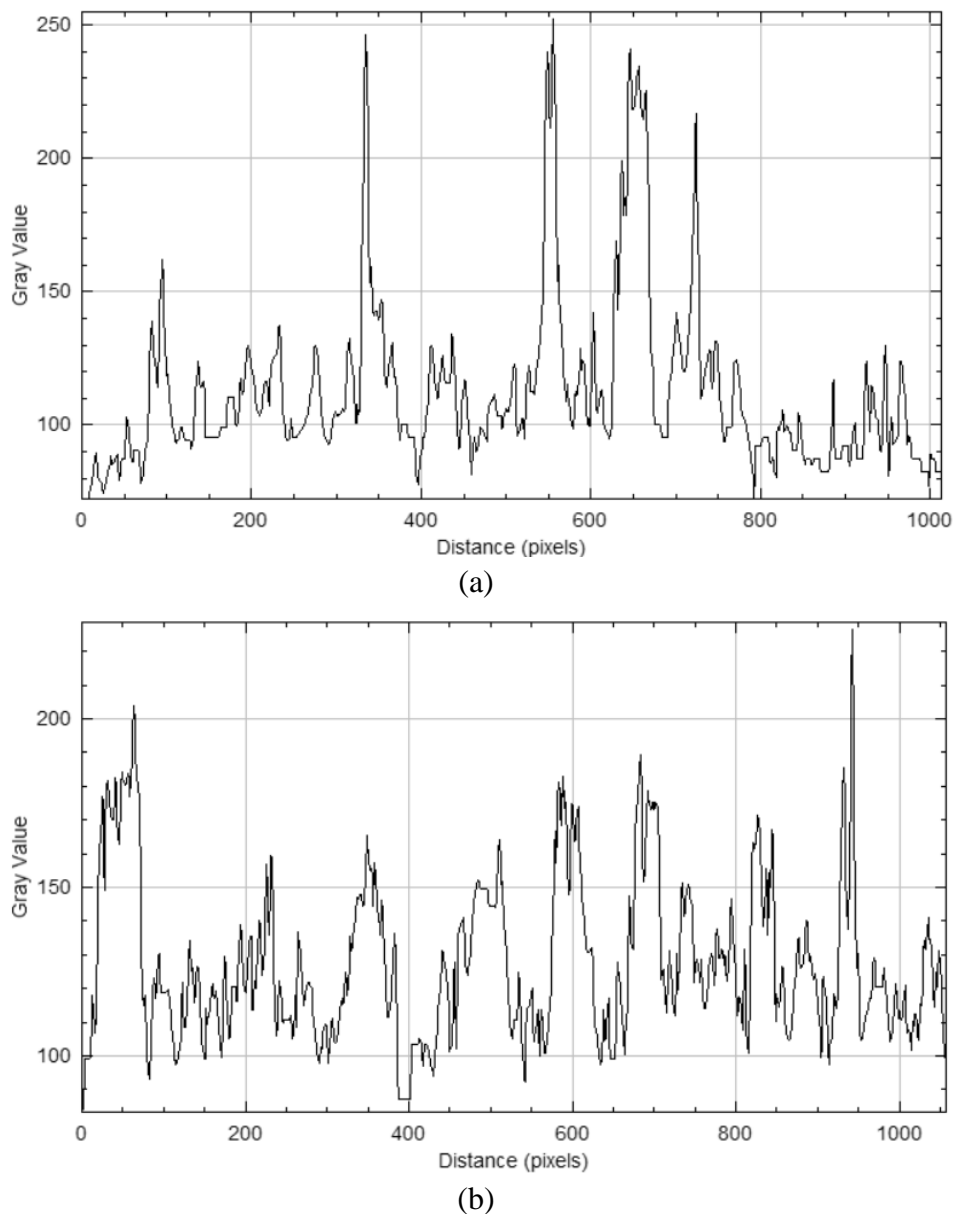


Fig. 27. The profilogram of the GFRPC surface after cutting (a) coarse, (b) fine

The cut quality of a material was evaluated by studying the R_a and R_q values of a surface. The mean values of R_a and R_q of all FRC used in the experiment are listed in the Table. 6. From each sample, four values of R_a and R_q were measured, then the mean values of those values were calculated and listed in Table 6. R_q values are more sensitive to variations on the surface compared to R_a values.

Table 6. Materials and the surface roughness values

Composite	Cutting type	R_q (μm)	R_a (μm)
AFRPC	Coarse	47.46948	23.07683
	Fine	42.77043	19.65323
BFRPC	Coarse	57.24038	32.9586
	Fine	57.24038	30.6312
CFRPC	Coarse	45.55205	19.90295
	Fine	41.05668	16.1255
GFRPC	Coarse	50.9088	23.65503
	Fine	46.81468	20.2816

From the final values of R_a and R_q calculated using ImageJ, it is visible that all the composites have the same trend on surface roughness depending on the cutting style. Among all the values, BFRPC has the highest values for both fine and coarse cutting. This value indicates that the quality of cuts on BFRPC samples is the lowest compared to all other samples. Even though the fine cutting value is less than the coarse cutting value, this indicates that the fine cutting gives better quality than the coarse cutting. In the case of AFRPC, like BFRPC, the fine cutting has less surface roughness than the coarse cutting, which is normal and shows that the fine cutting has a good quality of cut. Every sample of other composites exhibited the same trend, that the R_a and R_q values of fine cutting show a lesser value than coarse cutting, which means that fine cutting provides better performance in every sample. Compared with BFRPC, every composite, including BFRPC, followed the same trend in surface roughness analysis. Fig. 27 shows the graphical representation of the R_a and R_q values of both cuttings.

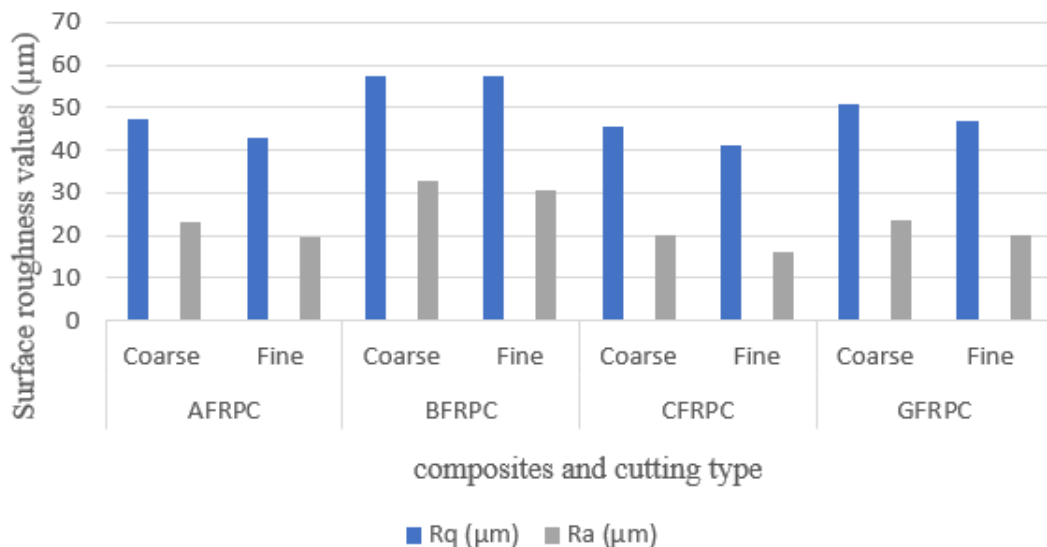


Fig. 28. Surface roughness values of composite samples with cutting type

3.3. Kerf Angle Value

The Kerf angle is one of the major parameters in analysing the quality of cutting using AWJM of composite materials. In this experiment, two types of cutting were carried out, one with a 50 mm/s feed rate called fine cutting and another one is coarse cutting with a 70 mm/s feed rate. The importance of the feed rate is that the taper angle varies with the feed rate of the cutting machine. The angles formed at the edges of the cut are called kerf taper angles. These angles occur as a result of the energy variation of the water jet throughout the cut. Normally, the angles will be higher at the top of the cut. Due to this energy difference, the kerf width is also higher at the top and lower at the bottom of the cut. Using the difference in kerf angle, it is easy to analyse the cut quality difference in the cut between the cuttings. Because for fine cutting the feed rate is less compared to the coarse cutting feed rate, therefore the value of kerf angle is also less than the kerf angle value of coarse cutting. The kerf angle values for all the composite samples are shown in the Figs. 28 to 31. Fig. 28 shows the kerf angles of BFRPC samples for coarse and fine cutting. Both angles show good values according to the cuttings. However, it was hard to measure the kerf angle on BFRPC due to defects at the corners of the cut, especially the presence of delamination. From the kerf angle values, the quality is good for both cutting since it shows a higher value (10.56 °) for coarse cutting and a lower value (3.4946 °) for fine cutting. Fig. 29 shows the kerf angles of CFRPC samples for coarse and fine cutting. In the case of CFRPC, the cuts look so perfect and do not exhibit any special changes on the edges other than taper angles. Due to this, the measurement of the kerf angle was easier and provided very good results. CFRPC also exhibited the same pattern as the BFRPC samples. Higher value (11.3099 °) for coarse and lower value (8.9525 °) for fine cutting. Fig. 30 shows the kerf angles of AFRPC samples for coarse and fine cutting. Both angles look good and do not show any special difference from the kerf taper angles. But the presence of delamination and fiber pullout is visible here. The values of angles show the same trend as BFRPC samples, and a higher value (6.0780Deg) for a coarse cutting sample and a lower value (5.1539 °) for fine cutting. Fig. 31 shows the kerf angles of GFRPC samples for coarse and fine cutting. GFRPC samples also show very good cutting results, but they also exhibited evidence of delamination on the edges, as in BFRPC. The kerf angles also followed the same result as the other composites, with a change only in the numerical values. In general, by analysing the values obtained all composites have good cutting quality according to the kerf angle values.

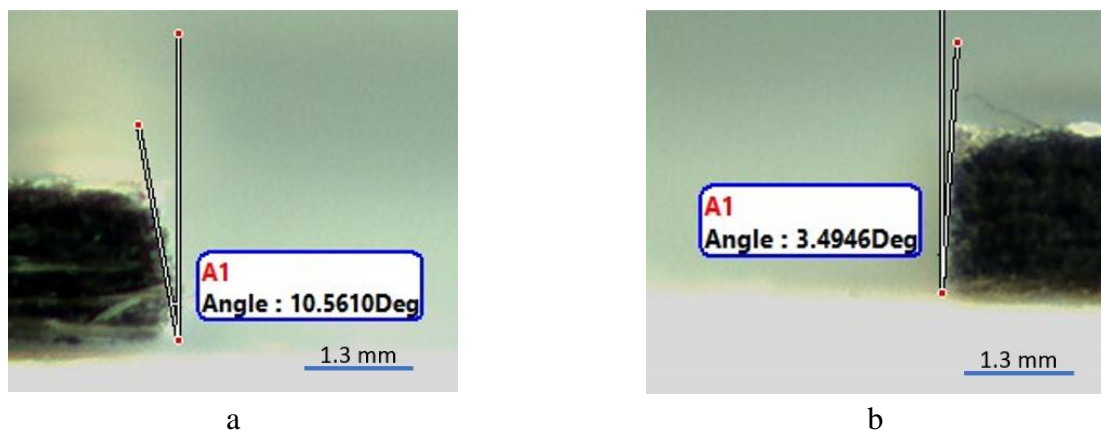


Fig. 29. Kerf taper angle values of BFRPC samples, coarse cutting (70mm/s) (a) and fine cutting (50 mm/s) (b) with 1.3× magnification

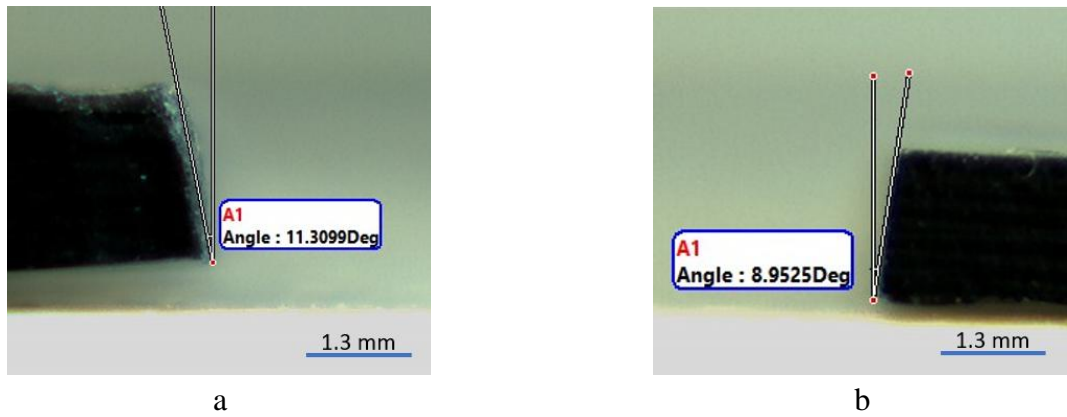


Fig. 30. Kerf taper angle values of CFRPC samples, coarse cutting (70mm/s) (a) and fine cutting (50 mm/s) (b) with 1.3× magnification

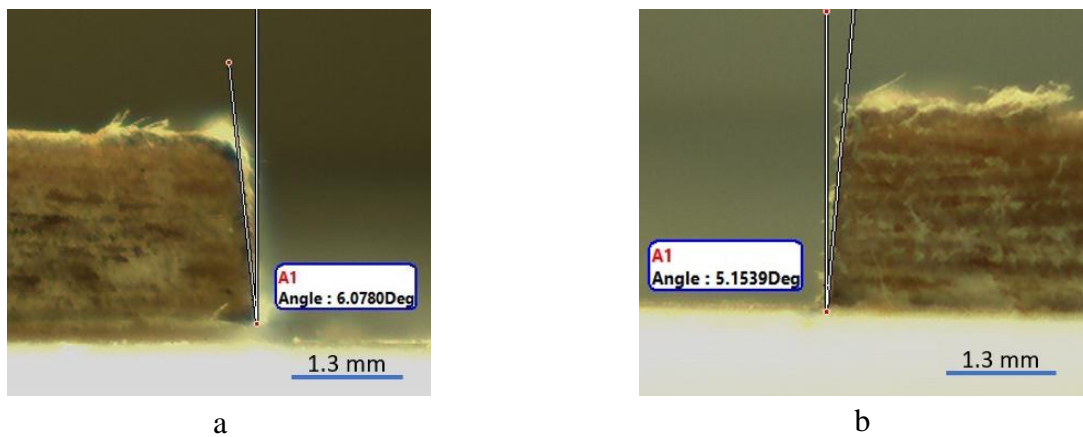


Fig. 31. Kerf taper angle values of AFRPC samples, coarse cutting (70 mm/s) (a) and fine cutting (50 mm/s) (b) with 1.3× magnification

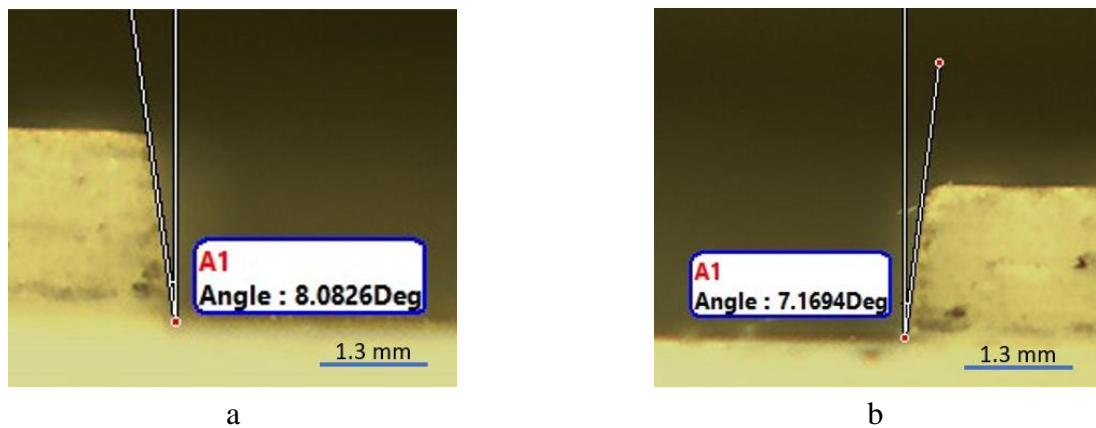


Fig. 32. Kerf taper angle values of GFRPC samples, coarse cutting (70 mm/s) (a) and fine cutting (50 mm/s) (b) with 1.3× magnification

Fig. 32 shows the mean kerf angle values for both coarse and fine cuttings. In every specimen, the kerf angle values follow the common pattern that the values are less for fine cutting and are higher for coarse cutting. From these values, the quality of cutting shows a good result since the value of angles shows the normal pattern. Even though fine cuttings in every sample have better cutting quality than coarse cuttings, because the delamination and other micro defects are less in fine cut samples than coarse cut samples.

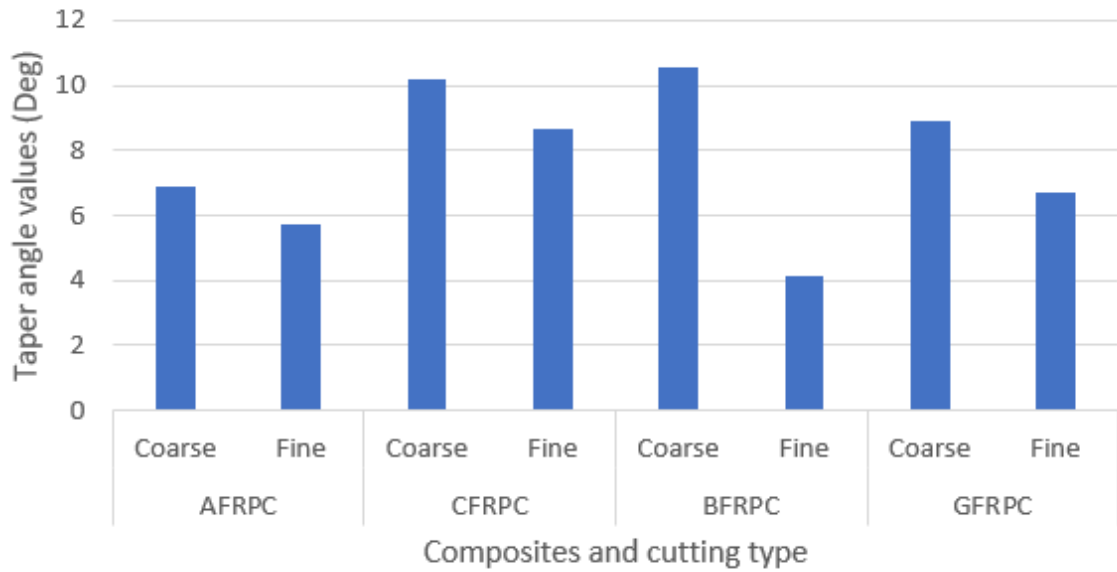


Fig. 33. Kerf taper angle values of composite samples with cutting type

By comparing the kerf angle values of BFRPC with other FRPC kerf angle values, BFRPC has the highest value of kerf angles for coarse cutting. The mean value of the coarse kerf angle of BFRPC is 10.56° and the fine kerf angle is 4.14° , which is the lowest value among all values. Compared to the mean coarse cutting values of other samples with BFRPC, the second highest value is for CFRPC, which is 10.21° , almost closer to the value of BFRPC. AFRPC and GFRPC have mean coarse cutting values of 6.89° and 8.89° , respectively. From all these values and comparing them with the BFRPC values, AFRPC has the lowest value. From the mean fine kerf angle values of the samples, the CFRPC value is 8.63° , which is more than twice the BFRPC value. The GFRPC and AFRPC are 6.69° and 5.73° , respectively, and these values are not higher than the value of the fine kerf angle of BFRPC.

3.4. Texturing On Composites

The effect of texturing on samples with varying feed rate and SOD were listed in Table 7. The values of kerf width of cuts are also listed in Table 7 to find out the difference between cutting and texturing. Moreover, pictures of samples with the texturing/cutting were also shown to analyze the results of the texturing. From Table 7 with the pictures of cut/ texturing samples, it is clear that the texturing effect is not really applicable to every composite using the Wazer desktop. In case of AFRPC, increasing the feed rate by keeping the SOD as constant results in texturing at a transverse speed of 250 mm/s. From 150 mm/s, the evidence of texturing was visible, even though at 250 mm/s, the almost form of texturing was exhibited. The CFRPC sample shows the texturing effect on feed rate of 70 mm/s and the SOD of 2.28 mm. Another situation where texturing was visible on CFRPC was the feed rate at 250 mm/s and SOD 9.12 mm. Even though in both situations the results were not very good, the texturing result was visible but not very deep, the feed rate was then increased to 300 mm/s and 350 mm/s, and better results were obtained. Fig. 23 shows the texturing result obtained on the CFRPC sample with feed rates of 300 and 350 mm/s. In all other situations, the cuts in the CFRPC sample are not visible and do not create any change. BFRPC samples exhibit inferior texturing results. From all those cuts and experiments, which were very difficult to attain, texturing on BFRPC samples. In the case of GFRPC, the results were the same as for BFRPC. On both of these composites, it is hard to obtain the texturing effect with the same values applied for AFRPC and CFRPC.

Table 7. Texturing on composite samples in different SOD and feed rate




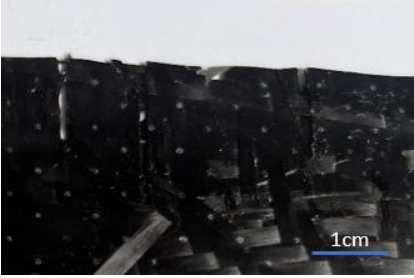
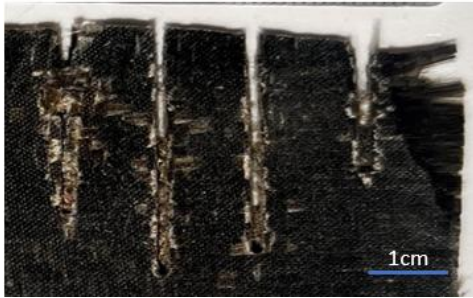

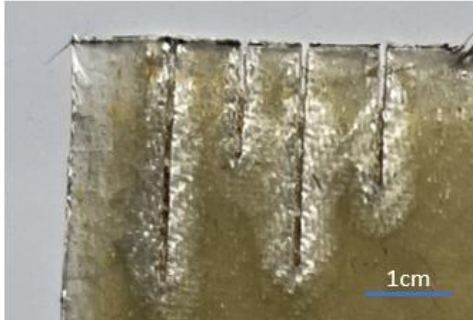
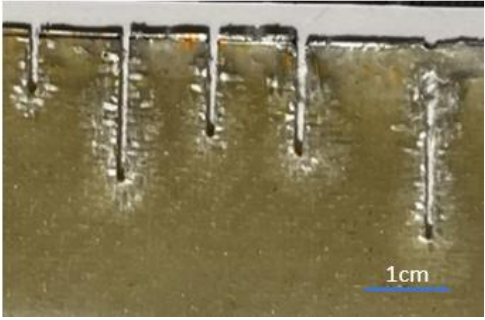
Samples	Increasing SOD (250 mm/s feed rate)	Increasing feed rate (2.28 SOD)
AFRPC		
CFRPC		
BFRPC		
GFRPC		

Table 8. Texturing effect for composites increasing feed rate with constant SOD (2.28mm SOD)

Feed rate (mm/s)	Texturing result			
	BFRPC	AFRPC	CFRPC	GFRPC
70	No	No	Texturing	No
100	No	Mild effect	No	No
150	No	Mild effect	No	No
200	No	Texturing started	No	No
250	No	Texturing	No	No

Table 9. Texturing effect for composites increasing SOD with constant feed rate (250mm/s)

SOD (mm)	Texturing result			
	BFRPC	AFRPC	CFRPC	GFRPC
2.28	No	Texturing	No	No
4.56	No	Texturing	No	No
6.84	No	Texturing	No	No
9.12	No	Texturing	Texturing	No

In Tables 8 and 9, the visual examination of the texturing effect on composites is listed. From the results, GFRPC and BFRPC have a texturing effect in both conditions, while AFRPC has a more texturing effect in different SOD. CFRPC achieved texturing at only two conditions when the SOD was 9.12 mm and the transverse speed was 250mm/s. But BFRPC shows texturing in all SOD with a constant feed rate of 250mm/s. The BFRPC and GFRPC samples did not show any texturing effect during the experiment. This means that it is hard to obtain texturing on these composites very easily using AWJM on the *Wazer desktop*. The maximum feed rate applied to the samples was 250 mm/s, and then it increased to 300 and 350 mm/s to examine the results, because increasing the feed rate of the cuts with constant SOD (2.28mm) sometimes exhibited more better results instead of increasing the SOD by keeping the feed rate as a constant (250mm/s). From the feed rates of 300 and 350 mm/s, CFRPC samples gave very good results of texturing. The AFRPC sample also gave good results for those 300 and 350 mm/s feed rate values. Whereas the GFRPC and BFRPC samples gave poor results, which were not even close to the texturing effect. Fig. 33 shows the result of the CFRPC sample with good results, and Fig. 34 shows the results of AFRPC, which is also a good texturing result. Figs. 35 and 36 show the results of BFRPC and GFRPC, respectively, then texturing process was unsuccessful.

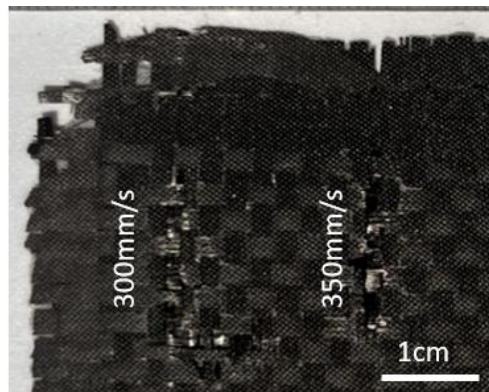


Fig. 34. CFRPC sample with cuts of feed rates of 300 mm/s and 350 mm/s

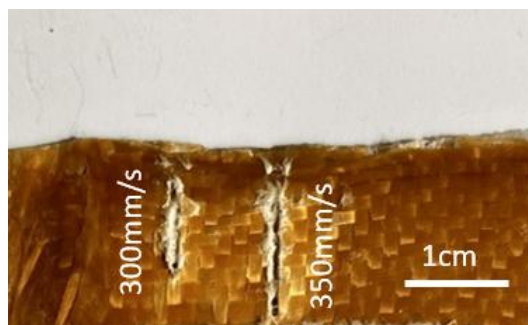


Fig. 35. AFRPC sample with cuts of feed rates of 300 mm/s and 350 mm/s

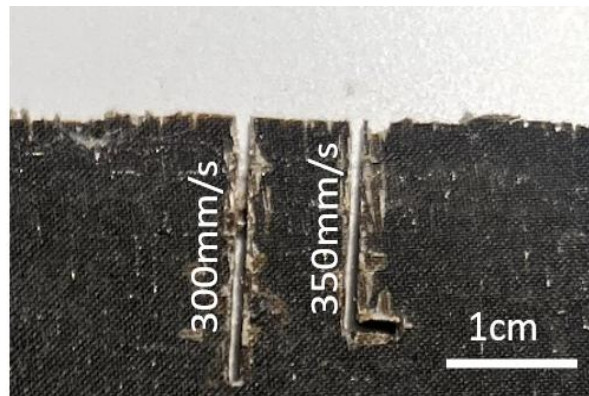


Fig. 36. BFRPC sample with cuts of feed rates of 300mm/s and 350mm/s

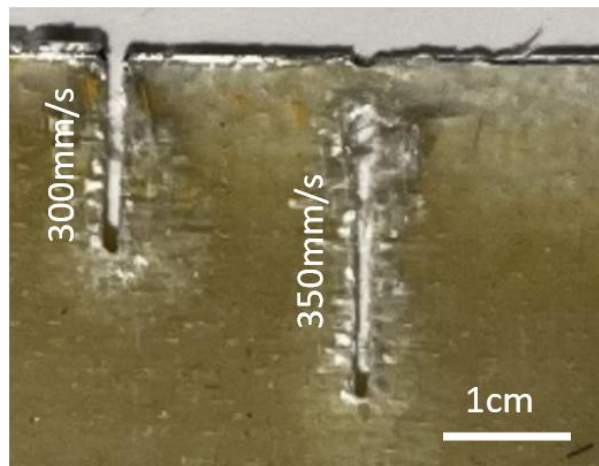


Fig. 37. GFRPC sample with cuts of feed rates of 300 mm/s and 350 mm/s

Tables 10 to 17 show the values of the upper and lower kerf widths of four composites. These values are taken to understand whether the cuts with varying parameters in the sample results in texturing or not. If the upper kerf width has a value and the lower kerf width value of any cutting remains zero, which indicates the texturing result. From the tables of AFRPC and CFRPC, the texturing results are visible since there are positive values for the upper and zero values for the lower kerf. If both kerfs show numerical values, such as in the GFRPC and BFRPC tables, that show that those marks are ended as cutting. In Tables 12 and 13, there are zero values for both kerf widths because the cutting action could not create any change on the surface of the CFRPC sample. In Tables 14,15,16, and 17, there are positive values for both kerf widths, which are examples of cut results. From all the tables and values, it is clear that the AFRPC and CFRPC result in texturing, and BFRPC and GFRPC could not result in texturing using Wazer desktop AWJM.

Table 10. Values of the upper and lower kerf width of AFRPC for increasing feed rate at 2.28mm SOD

Transverse speed (mm/s)	Upper kerf width (μm)	Lower kerf width (μm)
70	572.79	312.60
100	406.38	0
150	356.26	0
200	349.36	0
250	312.15	0

Table 11. Values of the upper and lower kerf width of AFRPC for increasing SOD at 250mm/s feed rate

SOD	Upper kerf width (μm)	Lower kerf width (μm)
2.28	312.15	0
4.56	324.45	0
6.84	361.47	0
9.12	400.58	0

Table 12. Values of the upper and lower kerf width of CFRPC for increasing feed rate at 2.28mm SOD

Feed rate (mm/s)	Upper kerf width (μm)	Lower kerf width (μm)
70	449.03	0
100	0	0
150	0	0
200	0	0
250	0	0

Table 13. Values of the upper and lower kerf width of CFRPC for increasing SOD at 250mm/s feed rate

SOD	Upper kerf width (μm)	Lower kerf width (μm)
2.28	0	0
4.56	0	0
6.84	0	0
9.12	657.63	0

Table 14. Values of the upper and lower kerf width of GFRPC for increasing feed rate at 2.28mm SOD

Feed rate (mm/s)	Upper kerf width (μm)	Lower kerf width (μm)
70	626.13	505.16
100	621.97	493.05
150	609.55	451.02
200	590.27	441.63
250	623.26	438.56

Table 15. Values of the upper and lower kerf width of GFRPC for increasing SOD at 250mm/s feed rate

SOD	Upper kerf width (μm)	Lower kerf width (μm)
2.28	623.26	360.08
4.56	579.75	349.56
6.84	589.74	336.34
9.12	567.65	320.15

Table 16. Values of the upper and lower kerf width of BFRPC for feed rate at 2.28mm SOD

Feed rate (mm/s)	Upper kerf width (μm)	Lower kerf width (μm)
70	525.15	477.39
100	525.43	433.37
150	528.66	417.22
200	531.31	410.35
250	576.47	380.08

Table 17. Values of the upper and lower kerf width of BFRPC for increasing SOD at 250mm/s feed rate

SOD	Upper kerf width (μm)	Lower kerf width (μm)
2.28	576.47	380.08
4.56	578.58	359.55
6.84	580.59	356.34
9.12	595.34	350.12

3.5. Kerf Angle Calculation of Texturing

The kerf angles of the texturing experiment were not very easy to measure using optical microscopes. So the only possible way to measure those values was the manual calculation using Eq. 1 for measuring the kerf angles of cuttings. Using these values, the quality of the cut can be examined.

The thickness of each FRPC material was different. The thickness of CFRPC was 2 mm and that of BFRPC was 1.61 mm. The thickness values for AFRPC and GFRPC were 3.32 mm and 1.76 mm respectively. These thickness values and the kerf width values, the value of kerf angle was calculated according to Equation 1. The calculated values are listed in Tables 18 and 19.

Table 18. Texturing effect for composites increasing feed rate at 2.28mm SOD

Feed rate(mm/s)	Kerf angle value (Deg)			
	BFRPC	AFRPC	CFRPC	GFRPC
70	0.852	2.240	6.431	1.976
100	1.641	0	0	2.098
150	1.987	0	0	2.528
200	2.153	0	0	2.491
250	3.544	0	0	3.055

Table 19. Texturing effect for composites increasing SOD at 250mm/s feed rate

SOD (mm)	Kerf angle value (Deg)			
	BFRPC	AFRPC	CFRPC	GFRPC
2.28	3.501	0	0	3.169
4.56	3.893	0	0	3.556
6.84	4.012	0	0	3.625
9.12	4.334	0	9.37	3.918

From calculating the kerf angle values, the values are different for all FRPC because the kerf width values and the thickness values are different for all samples. From the values of AFRPC, there was only one time the kerf angle value was positive, and it was 2.24° , which is the only situation in which the texturing was not visible in FRPC during the texturing experiment. The values of CFRPC showed two positive values, which are 6.431° at constant SOD (2.28mm) and feed rate of 70mm/s and 9.37° at constant feed rate 250 mm/s and SOD of 9.12 mm. During both conditions, the texturing was visible. From the results of BFRPC it shows a clear trend of increasing the kerf angle values in both conditions with increasing the SOD by increasing the feed rate and constant and increasing the feed rate by keeping the SOD as a constant. GFRPC also exhibited the same pattern, followed by BFRPC. And all these values indicate that the quality of processing is good because the kerf angles are small

for low feed rate and low SOD values, and it increases with increasing any of the parameters, whether it is the SOD or feed rate of AWJM.

3.6. Cutting Cost Calculation

To estimate the cost of cutting using AWJM for all FRPCs, a few parameters and formulas were used. The cutting cost for fine and coarse cutting of each sample per one cutting operation was calculated using these parameters and equations. For the calculations, the cutting parameters such as job (cutting) time, amount of abrasive used, and cutting feed rate were taken from the official online platform *Wazer Desktop* AWJM. Other parameters, such as the cost of electricity, the cost of water, and the price of abrasive, are taken from the Internet. Table 20 shows the cut cost calculations for cutting FRPCs.

Table 20. Cutting cost

Composite	Cutting type (feed rate) (mm/min)	Job time (h)	Abrasive used (kg)	Abrasive cost (euro)	Cut cost (euro)
CFRPC	Coarse (70)	0.0405	0.37	1.37	0.178
	Fine (50)	0.0544	0.49	1.77	0.236
AFRPC	Coarse (70)	0.0405	0.37	1.37	0.178
	Fine (50)	0.0544	0.49	1.77	0.236
GFRPC	Coarse (70)	0.0405	0.37	1.37	0.178
	Fine (50)	0.0544	0.49	1.77	0.236
BFRPC	Coarse (70)	0.0405	0.37	1.37	0.178
	Fine (50)	0.0544	0.49	1.77	0.236

AWJM cutting costs are calculated using the formula

$$C_{\text{cut}} = C_{\text{abrasive}} + C_{\text{electricity}} + C_{\text{water used}}, \quad (4)$$

where: C_{cut} is the cost of cutting (€); C_{abrasive} is the cost of abrasive used; $C_{\text{electricity}}$ is the cost of electricity, and $C_{\text{water used}}$ is the cost of water used.

Abrasive cost can be calculated by the equation

$$C_{\text{abrasive}} = W_A \times C_A, \quad (5)$$

where: W_A is the abrasive consumption (kg), C_A is the cost per kg. The abrasive used in the *Wazer Desktop* is 80-Mesh Alluvial Garnet, and the cost per kg is 2.8 euros.

Electricity cost can be calculated by the equation:

$$C_{\text{electricity}} = W_E \times C_E, \quad (6)$$

where: W_E is the electrical power consumption (h), and C_E is the unit price of electricity (kWh). *Wazer Desktop* consumes 1.5 kW of power for operations. The approximate cost of power per unit is 0.45 euros/hour.

Water cost can be calculated by the equation:

$$C_{\text{water used}} = W_W \times C_W, \quad (7)$$

where W_W is the water consumption (m^3/h), and C_W is the unit price of water (liters). The water consumption rate of the *Wazer Desktop* is 0.95 lit/min, and the approximate cost of water in Lithuania is 0.00175 EUR/liter.

The calculation of the cut cost values shows the same pattern, as the parameters and all other values are the same for the same form of cutting. The fine cutting value is higher compared to the coarse cutting values. During the fine cutting operation, the feed rate of the *Wazer Desktop* AWJM is 50 mm/s, which is lower than the coarse cutting feed rate (70mm/s). This difference in feed rate has a major impact on increasing the fine cutting cost. Due to the lower speed of the nozzle, the machine requires more time to finish the cutting job. During all this time, the machine is pumping water and using abrasives and electricity. The job time required for finishing the fine cutting operation is almost 29% higher than the time required for finishing the coarse cutting. The amount of abrasive used is also 27% higher than in the fine cutting process. Due to the high amount of abrasive usage, the abrasive cost is also increased by more than 25%. Overall, there is a 32% difference in the cutting costs of fine and coarse cuttings.

3.7. Chapter Summary

Samples of the composite cuts were examined with two optical microscopes and the quality of the cut. Using ImageJ software, a surface profile of each sample was made and the data analysed. In addition, surface roughness values were calculated and the result was that fine cutting produces a better cut quality for all composites than coarse cutting. After measuring the taper angles, it was realised that the angles of the fine-cut taper angles are always smaller than those of the coarse-cut taper angles, as is usual. The texturing effect is studied by measuring the taper edge widths of the top and bottom of cuts and finding the composites with texturing effects, which are CFRPC and AFRPC. The cost of the cutting of all the samples is also calculated

4. Environmental and Economic Impacts of the Application of AWJM

4.1. Environmental Impacts

Compared to other cutting methods, which can be conventional or nonconventional, AWJM has a priority over any other method since it uses a water jet as a cutting tool. A high-pressure water jet is pumped with the help of a narrow nozzle to cut the materials, therefore, AWJM is highly environmentally friendly compared to any other method. In AWJM, the use of water does not produce any harmful byproducts, such as heat and toxic gases, during the operation of the machine, which also makes the AWJM method more sustainable and eco-friendly [54]. Even though one concern about AWJM is the amount of water usage, because AWJM uses a high amount of water for the machining operations, even if it is a cutting, drilling, or milling process [55]. Due to this, the higher scale application of AWJM in industries can create a harmful impact on the water sources based on the water supply in the regions. The reuse of water is a possible solution to avoid such an impact. But during this situation, the major issue related to this machine is that even if the water is completely reusable, the abrasive particles are not at all because of some reasons. That is another harmful environmental concern with the use of AWJM [56]. Even though the waste production in the AWJM process is less compared to other methods, the major waste material produced during the AWJM operation is the used abrasive particles. The abrasive particles during the operation will be mixed with the water and material waste produced during the operation. Due to this, the abrasive particles once used are not reusable, making them permanent waste, and are mostly not recyclable [56]. But there are studies about the use of recycled abrasive particles; still, the recycled particles do not produce the same result as new market abrasive particles [56]. The usage of energy for AWJM operations is also one of the concerns related to the environment, because they are machines operated with high-pressure water pumps and some other machine parts, which consume a huge amount of energy. Among all these concerns, one of the major advantages of AWJM is the absence of a heat-affected zone during any operation of AWJM. This is a permanent advantage of AWJM because the cutting tool is water, which does not produce heat during machining operations. This makes it environmentally friendly because overall, the chances of thermal damage due to machining are much less in AWJM operations [57].

4.2. Economic Impacts

AWJM is a modern method with lots of advantages since it uses modern technology therefore, the initial cost for the AWJM machine will be higher. AWJM uses numerous costly parts inside the machine, such as high-pressure pumps. Therefore, the price of AWJM machines is not very cheap. But for large industries, these initial investments are negligible when compared with the results produced by AWJM and the operational ease of AWJM [58]. Even though AWJM is a modern technology, the operation of these machines is not very hard; a good training is enough to learn the operating setup of these machines. This training in learning about the machine can come at a price in terms of the economic impacts of AWJM. AWJM has an advantage that it is a machine that a part of the operation only needs the control of an operator, after that, the machine will perform the remaining part itself, which can reduce the cost for the machine operator. Still, operator control is necessary for the maintenance and cleaning of the machine. The use of abrasive particles can make the operational cost of AWJM a bit higher; at the same time, the cutting tool is water, which makes it less costly for the cutting tool. The abrasive materials once used are not reusable, which costs more amount of money for abrasive particles. One of the advantages of AWJM is that the less wastage of material,

which helps to save cost on materials, and the high and precise cutting quality of this machine avoids secondary processing, which is also very helpful for cost saving [59].

4.3. Chapter Summary

From the analysis of the environmental and economic impacts of AWJM is one of the effective cutting methods available in the market for machining of composites. The major advantages of AWJM are the cost savings by reducing the unwanted maintenance and a zero-cost cutting tool. But the abrasive waste production in AWJM is a strong environmental concern. Even though AWJM is one of the modern sustainable cutting methods suggested by researchers these days for machining of composites, due to the noticeable advantages of AWJM, such as environmentally friendly machining, low waste production during the operations, and no heat-affected zone production. Moreover, AWJM is suitable for producing complex geometries with high precision.

Conclusions

1. Two types of cutting in four composite laminate specimens (BFRPC, GFRPC, CFRPC, and AFRPC) showed that, regardless of the material tested and the speed of the cutting feed rate, which varied between 50 mm/s and 70 mm/s, the AWJM provided a very good cutting quality and surface finish. Comparing the results of BFRPC with those of the other composites studied, it was found that BFRPC showed delamination after cutting, as was the case for AFRPC and GFRPC. No delamination was observed only in the case of CFRPC. Comparing the Kerf taper angle values with other composites, BFRPC has the highest value for coarse cutting and the lowest value for fine cutting. All other composite laminates had the same Kerf taper angle values, low values for fine cutting, and high values for coarse cutting. In the case of surface roughness values, also BFRPC has the highest values for both R_a and R_q among all FRC.
2. The surface texturing analysis of the composite laminates showed, that for each composite studied, different feed rate and SOD parameters are required to obtain the texturing effect. With the selected feed rate and the SOD parameters, only CFRPC and AFRPC achieved a texturing effect. The texturing effect was determined by measuring the upper and lower (if cut was obtained) Kerf width values of the textures. For the CFRP composite laminate, the texturing result was obtained at a feed rate of 70 mm/s and a SOD of 2.28 mm and at a feed rate of 250 mm/s and a SOD of 9.12 mm. For AFRPC, texture was produced in all cases tested except at 70 mm/s feed rate and 2.28 mm SOD. However, no texturing effect was obtained in the case BFRPC and GFRPC.
3. Cost analysis of cutting composite laminates shows that coarse cuts at a feed rate of 70 mm/s are 32% more cost effective than fine cuts at a feed rate of 50 mm/s. This is due to the reduction in working time. In addition, coarse cutting uses fewer abrasive particles compared to fine cutting. This can reduce the environmental impact by reducing operating costs and waste after the machining process.

List of References

1. SATHISHKUMAR, T.P., SATHEESHKUMAR, S. and NAVEEN, J., 2014. Glass Fiber-Reinforced Polymer Composites—a Review. *Journal of Reinforced Plastics and Composites*, vol. 33, no. 13, pp. 1258–1275.
2. SABA, N., et al, 2016. Recent Advances in Epoxy Resin, Natural Fiber-Reinforced Epoxy Composites and their Applications. *Journal of Reinforced Plastics and Composites*, vol. 35, no. 6, pp. 447–470.
3. ANU KUTTAN, A., RAJESH, R. and DEV ANAND, M., 2021. Abrasive Water Jet Machining Techniques and Parameters: A State of the Art, Open Issue Challenges and Research Directions. *Journal of the Brazilian Society of Mechanical Sciences and Engineering*, vol. 43, pp. 1–14.
4. CHEN, A.Y., et al, 2021. Carbon-Fiber Reinforced Polymer Composites: A Comparison of Manufacturing Methods on Mechanical Properties. *International Journal of Lightweight Materials and Manufacture*, vol. 4, no. 4, pp. 468–479.
5. MORAMPUDI, P., et al, 2021. Review on Glass Fiber Reinforced Polymer Composites. *Materials Today: Proceedings*, vol. 43, pp. 314–319.
6. ZHANG, B., et al, 2021. Surface and Interface Modification of Aramid Fiber and its Reinforcement for Polymer Composites: A Review. *European Polymer Journal*, vol. 147, pp. 110352.
7. CHOWDHURY, I.R., PEMBERTON, R. and SUMMERSCALES, J., 2022. Developments and Industrial Applications of Basalt Fibre Reinforced Composite Materials. *Journal of Composites Science*, vol. 6, no. 12, pp. 367.
8. SINGH, Y., et al, 2022. Process Parameter Optimization in Laser Cutting of Coir Fiber Reinforced Epoxy Composite-a Review. *Materials Today: Proceedings*, vol. 48, pp. 1021–1027.
9. LEONE, C., MINGIONE, E. and GENNA, S., 2021. Laser Cutting of CFRP by Quasi-Continuous Wave (QCW) Fibre Laser: Effect of Process Parameters and Analysis of the HAZ Index. *Composites Part B: Engineering*, vol. 224, pp. 109146.
10. LI, M., CHEN, L. and YANG, X., 2021. A Feasibility Study on High-Power Fiber Laser Cutting of Thick CFRP Laminates using Single-Pass Strategy. *Optics & Laser Technology*, vol. 138, pp. 106889.
11. KHAN, M.A., SONI, H., MASHININI, P.M. and UTHAYAKUMAR, M., 2021. Abrasive Water Jet Cutting Process Form Machining Metals and Composites for Engineering Applications: A Review. *Engineering Research Express*, vol. 3, no. 2, pp. 022004.
12. DAHIYA, A.K., BHUYAN, B.K. and KUMAR, S., 2021. Optimization of Process Parameters for Surface Roughness of GFRP with AWJ Machining using Taguchi and GRA Methods. *Int.J.Mod.Manuf.Technol.*, vol. 13, no. 2, pp. 2021.
13. WANG, M., et al, 2023. Investigation on the Machinability of SiCp/Al Composite by in-Situ Laser Assisted Diamond Cutting. *Journal of Materials Processing Technology*, vol. 318, pp. 118044.
14. SHARMA, A.K., et al, 2020. A Study of Advancement in Application Opportunities of Aluminum Metal Matrix Composites. *Materials Today: Proceedings*, vol. 26, pp. 2419–2424.
15. HAN, X., et al, 2021. On Understanding the Specific Cutting Mechanisms Governing the Workpiece Surface Integrity in Metal Matrix Composites Machining. *Journal of Materials Processing Technology*, vol. 288, pp. 116875.
16. ZHAO, G., et al, 2020. Micro-Milling of 65 Vol% SiCp/Al Composites with a Novel Laser-Assisted Hybrid Process. *Ceramics International*, vol. 46, no. 16, pp. 26121–26128.
17. WANG, Y., et al, 2019. Investigation on Cutting Mechanism of SiC P/Al Composites in Precision Turning. *The International Journal of Advanced Manufacturing Technology*, vol. 100, pp. 963–972.
18. SHIJIN, L.U., et al, 2021. Cutting Path-Dependent Machinability of SiCp/Al Composite Under Multi-Step Ultra-Precision Diamond Cutting. *Chinese Journal of Aeronautics*, vol. 34, no. 4, pp. 241–252.

19. YOU, K., et al, 2020. Advances in Laser Assisted Machining of Hard and Brittle Materials. *Journal of Manufacturing Processes*, vol. 58, pp. 677–692.
20. CIECIELAĞ, K., KEÇIK, K. and ZALESKI, K., 2020. Effect of Depth Surface Defects in Carbon Fibre Reinforced Composite Material on the Selected Recurrence Quantifications. *Advances in Materials Science*, vol. 20, no. 2, pp. 71–80.
21. CIECIELAĞ, K., ZALESKI, K. and KEÇIK, K., 2022. Effect of Milling Parameters on the Formation of Surface Defects in Polymer Composites. *Materials Science*, vol. 57, no. 6, pp. 882–893.
22. CIECIELAĞ, K., KEÇIK, K. and ZALESKI, K., 2020. Defects Detection from Time Series of Cutting Force in Composite Milling Process by Recurrence Analysis. *Journal of Reinforced Plastics and Composites*, vol. 39, no. 23-24, pp. 890–901.
23. GHOBADI, A., 2017. Common Type of Damages in Composites and their Inspections. *World Journal of Mechanics*, vol. 7, no. 2, pp. 24–33.
24. KEÇIK, K., CIECIELAĞ, K. and ZALESKI, K., 2017. Damage Detection of Composite Milling Process by Recurrence Plots and Quantifications Analysis. *The International Journal of Advanced Manufacturing Technology*, vol. 89, pp. 133–144.
25. KŁONICA, M., MATUSZAK, J. and ZAGÓRSKI, I., 2019. Effect of Milling Technology on Selected Surface Layer Properties. IEEE.
26. SHANMUGAM, D.K., CHEN, F.L., SIORES, E. and BRANDT, M., 2002. Comparative Study of Jetting Machining Technologies Over Laser Machining Technology for Cutting Composite Materials. *Composite Structures*, vol. 57, no. 1-4, pp. 289–296.
27. SHANMUGAM, D.K., NGUYEN, T. and WANG, J., 2008. A Study of Delamination on Graphite/Epoxy Composites in Abrasive Waterjet Machining. *Composites Part A: Applied Science and Manufacturing*, vol. 39, no. 6, pp. 923–929.
28. D.K. Shanmugam, T. Nguyen, J. Wang, A study of delamination on graphite/ epoxy composites in abrasive water jet machining, *Compos.: Part A* 39 (2008) 923–929, <https://doi.org/10.1016/j.compositesa.2008.04.001>.
29. PRASAD, K.S. and CHAITANYA, G., 2019. Analysis of Delamination in Drilling of GFRP Composites using Taguchi Technique. *Materials Today: Proceedings*, vol. 18, pp. 3252–3261. Dhanawade, A., Kumar, S., Kalmekar, R. V., (2016). Abrasive Water Jet Machining of Carbon Epoxy Composite, *Def. Sci. J.*, 66 (5), 522-528. DOI : 10.14429/dsj.66.9501
30. HASHISH, M., 2024. Abrasive Waterjet Machining. *Materials*, vol. 17, no. 13, pp. 3273.
31. Dhanawade, A., Kumar, S., Kalmekar, R. V., (2016). Abrasive Water Jet Machining of Carbon Epoxy Composite, *Def. Sci. J.*, 66 (5), 522-528. DOI : 10.14429/dsj.66.9501
32. MayuetAres, P. F., Mata, F.G., Ponce, M. B., Gomez, J.S., (2019) Defect Analysis and Detection of Cutting Regions in CFRP Machining Using AWJM. *Materials*, 12(24), 1-15. <https://doi.org/10.3390/ma12244055>
33. YOUSSEF, H.A., EL-HOFY, H.A., ABDELAZIZ, A.M. and EL-HOFY, M.H., 2021. Accuracy and Surface Quality of Abrasive Waterjet Machined CFRP Composites. *Journal of Composite Materials*, vol. 55, no. 12, pp. 1693–1703
34. JEYKRISHNAN, J., et al, 2019. Optimization of Process Parameters in Abrasive Water Jet Machining/Cutting (AWJM) of Nickel Alloy using Traditional Analysis to Minimize Kerf Taper Angle. *Materials Today: Proceedings*, vol. 16, pp. 392–397.
35. HLAVÁČ, L.M., 2009. Investigation of the Abrasive Water Jet Trajectory Curvature Inside the Kerf. *Journal of Materials Processing Technology*, vol. 209, no. 8, pp. 4154–4161.
36. LI, M., et al, 2021. Study on Kerf Characteristics and Surface Integrity Based on Physical Energy Model during Abrasive Waterjet Cutting of Thick CFRP Laminates. *The International Journal of Advanced Manufacturing Technology*, vol. 113, pp. 73–85.
37. ZENG, J. and HENNING, A., 2009. Kerf Characterization in Abrasive Waterjet Cutting.
38. CASTRO-CASADO, D., 2021. Chemical Treatments to Enhance Surface Quality of FFF Manufactured Parts: A Systematic Review. *Prog Addit Manuf* 6: 307–319. DOBES, J., et al, 2017.

- Effect of Mechanical Vibration on Ra, Rq, Rz, and Rt Roughness Parameters. *The International Journal of Advanced Manufacturing Technology*, vol. 92, pp. 393–406.
39. AZMIR, M.A. and AHSAN, A.K., 2009. A Study of Abrasive Water Jet Machining Process on Glass/Epoxy Composite Laminate. *Journal of Materials Processing Technology*, vol. 209, no. 20, pp. 6168–6173.
 40. AZMIR, M.A. and AHSAN, A.K., 2008. Investigation on Glass/Epoxy Composite Surfaces Machined by Abrasive Water Jet Machining. *Journal of Materials Processing Technology*, vol. 198, no. 1-3, pp. 122–128.
 41. UNDE, P.D., et al, 2015. Experimental Investigations into Abrasive Waterjet Machining of Carbon Fiber Reinforced Plastic. *Journal of Composites*, vol. 2015, no. 1, pp. 971596.
 42. OBILOR, A.F., PACELLA, M., WILSON, A. and SILBERSCHMIDT, V.V., 2022. Micro-Texturing of Polymer Surfaces using Lasers: A Review. *The International Journal of Advanced Manufacturing Technology*, vol. 120, no. 1, pp. 103–135.
 43. RIVEIRO, A., et al, 2018. Laser Surface Texturing of Polymers for Biomedical Applications. *Frontiers in Physics*, vol. 6, pp. 16.
 44. HAMILTON, D.W., et al., 2006. Surface topography and cell behaviour. In: Encyclopedia of biomaterials and biomedical engineering Taylor and Francis New York. *Surface Topography and Cell Behaviour*, pp. 1–15.
 45. YAHYAVI ZANJANI, M., et al, 2019. Process Control in Jet Electrochemical Machining of Stainless Steel through Inline Metrology of Current Density. *Micromachines*, vol. 10, no. 4, pp. 261.
 46. SHEKAR, A.C., SAWALMEH, A., ZITOUNE, R. and HOF, L.A., 2025. Optimization of Surface Texturing Parameters in Additively Manufactured Continuous Fiber Composites using Abrasive Waterjet Technique for Composite Repair Applications. *Composites Part A: Applied Science and Manufacturing*, vol. 190, pp. 108698.
 47. THAKUR, R.K. and SINGH, K.K., 2021. Evaluation of Advanced Machining Processes Performance on Filler-Loaded Polymeric Composites: A State-of-the-Art Review. *Journal of the Brazilian Society of Mechanical Sciences and Engineering*, vol. 43, no. 6, pp. 300.
 48. XU, J., et al, 2023. A Review on CFRP Drilling: Fundamental Mechanisms, Damage Issues, and Approaches Toward High-Quality Drilling. *Journal of Materials Research and Technology*, vol. 24, pp. 9677–9707.
 49. HEJAJI, A., et al, 2016. Machining Damage in FRPs: Laser Versus Conventional Drilling. *Composites Part A: Applied Science and Manufacturing*, vol. 82, pp. 42–52.
 50. HEJAJI, A., et al, 2019. Influence of Controlled Depth Abrasive Water Jet Milling on the Fatigue Behavior of Carbon/Epoxy Composites. *Composites Part A: Applied Science and Manufacturing*, vol. 121, pp. 397–410.
 51. MAZARBHUIYA, R.M., DUTTA, H., DEBNATH, K. and RAHANG, M., 2020. Surface Modification of CFRP Composite using Reverse-EDM Method. *Surfaces and Interfaces*, vol. 18, pp. 100457.
 52. SHU, S., et al, 2025. A High Bonding Tensile Strength of CFRP Ultrafast Laser Surface Texturing Method for Surface Damage Repair. *Optics & Laser Technology*, vol. 180, pp. 111601.
 53. SOURD, X., ZITOUNE, R., CROUZEIX, L. and COULAUD, M., 2022. Influence of the Texturing Quality Consecutive to Abrasive Water Jet Machining on the Adhesive Properties in Mode I of 3D Woven Composite Assemblies. *Composites Part B: Engineering*, vol. 242, pp. 110091.
 54. PEREC, A., RADOMSKA-ZALAS, A., FAJDEK-BIEDA, A. and KAWECKA, E., 2022. Efficiency of Tool Steel Cutting by Water Jet with Recycled Abrasive Materials. *Materials*, vol. 15, no. 11, pp. 3978.

55. GUGLIELMI, G., et al, 2021. Life Cycle Environmental and Economic Comparison of Water Droplet Machining and Traditional Abrasive Waterjet Cutting. *Sustainability*, vol. 13, no. 21, pp. 12275.
56. BABU, M.K. and CHETTY, O.K., 2003. A Study on Recycling of Abrasives in Abrasive Water Jet Machining. *Wear*, vol. 254, no. 7-8, pp. 763–773.\
57. JANKOVIĆ, P., et al, 2015. Aspects of Machining Parameter Effect on Cut Quality in Abrasive Water Jet Cutting. *Applied Mechanics and Materials*, vol. 809, pp. 201–206.
58. JANI, S.P., KUMAR, A.S., KHAN, M.A. and JOSE, A.S., 2021. Design and Optimization of Unit Production Cost for AWJ Process on Machining Hybrid Natural Fibre Composite Material. *International Journal of Lightweight Materials and Manufacture*, vol. 4, no. 4, pp. 491–497.
59. BHOWMIK, S., Jagadish and RAY, A., 2017. Abrasive Water Jet Machining of Composite Materials. *Advanced Manufacturing Technologies: Modern Machining, Advanced Joining, Sustainable Manufacturing*, pp. 77–97.

Appendices

Appendix 1. Industrial Engineering : conference proceedings

*Proceedings of 12th International Young Researchers Conference
INDUSTRIAL ENGINEERING 2025*

Investigation of the effect of abrasive water jet machining parameters on basalt fiber reinforced epoxy composites

Sachinkumar MANCHERY SAJAN^{1*}, Kristina ŽUKIENĖ²

1 Department of Production Engineering, Kaunas University of Technology, Studentu 56, Kaunas 51424, Lithuania

2 Department of Production Engineering, Kaunas University of Technology, Studentu 56, Kaunas 51424, Lithuania

**sachinkumar.manchery@ktu.edu*

Abstract

Nowadays, the use of composites is very common in every industry. The reason behind this is the better properties of composites compared to traditional materials. Abrasive water jet machining (AWJM) is widely used in industry for composite materials. However, AWJM faces certain challenges when cutting composite materials, including delamination, fiber pull-out, matrix erosion, and the tapering of the cutting kerf. This paper presents an investigation of the effect of AWJM parameters on basalt fiber reinforced epoxy composites. The influence of the feed rate on the cutting quality of the samples was investigated. The responses of the machining process, such as kerf and roughness parameters, are measured and studied.

Keywords: Abrasive water jet, Composite, Cutting, Kerf, Roughness.

1. Introduction

Nowadays, the use of composites is very common in every industry. This is because composites have better properties than traditional materials, such as high strength-to-weight ratios, corrosion resistance, structural flexibility, low thermal conductivity, etc. [1]. There are two types of composites available on the market, synthetic and natural. The basalt fiber reinforced polymer composite is an example of a composite derived from a mineral source [2]. Basalt fibers are made from basalt rock by melting it and converting it into fiber [3]. The eco-friendly nature of this composite makes it a more sustainable option than many other composites [3]. Due to the wide use of composites, the machining of these materials is also becoming increasingly important these days [4]. There are numerous methods available in the market for cutting and other machining operations of composites. Among them, abrasive water jet machining (AWJM) has a higher priority due to the many advantages of this method [4]. In this paper, the use of AWJM is highlighted for the cutting of composite materials. To analyse the cutting quality, the kerf characteristics and roughness characteristics are measured and studied. This study aims to investigate the effect of AWJM parameters on basalt fiber reinforced epoxy composites.

2. Materials and methods

The basalt composite was produced by cutting 10 basalt fibre plies (Basaltex NV, Wevelgem, Belgium) with dimensions of 100 × 100 mm. A 7:3 mix of epoxy resin and hardener (R&G Faserverbundwerkstoffe GmbH, Epoxy Resin L, Hardener S) was used to prepare the composite. The epoxy resin is cold cured with a cure time of 24 hours. The composite was produced using a hand-lay-up technique with the support of the vacuum bagging technique. Composite samples with a dimension of 30 × 30 mm were cut using a Wazer desktop AWJM. 80-mesh alluvial garnet was used as the abrasive particle in the AWJM cutting operation. The abrasive rate was 0.15 kg/min. Two types of cuts were made: coarse (feed rate was 22 mm/min) and fine (feed rate was 10 mm/min). A cutting path is shown in Figure 1.

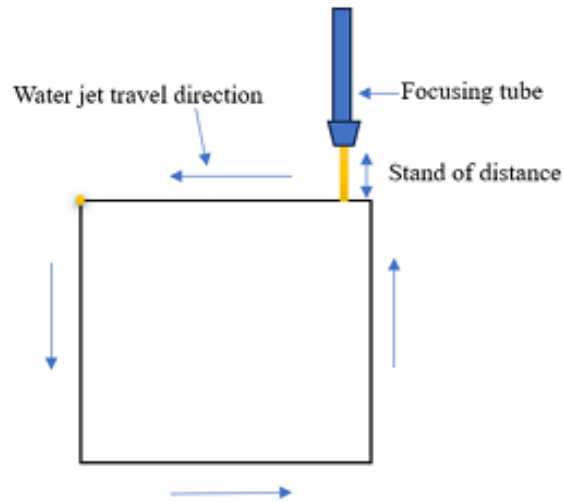


Fig. 1 Schematic of the cutting path

To investigate the quality of the cut, the samples were examined after cutting using a Nikon ECLIPSE LV100ND optical microscope. The images captured by this microscope were used to calculate the values of the roughness parameters of the cut surfaces. The roughness parameters calculated in this work are the arithmetic mean roughness (R_a) and the root mean square roughness (R_q). Parameters were calculated using ImageJ software. At least three cross-sectional profiles of the optical microscope images were used for the calculations and were extracted using ImageJ software. The system analyses the intensity of the grey variation on the cut surface along a selected line. The x-axis shows the length of the horizontal scan in pixels, and the y-axis shows the intensity of the grey. Peaks in the profile indicate high grey values, and valleys are low grey values.

Kerf angles were measured using the optical microscope "Moticam 1000 1.3M Pixel" and "Motic Images plus 2.0" software. The Kerf angles were calculated from four measurements. Using the same microscope, a qualitative study of the delamination images was carried out to investigate the presence of delamination after the cutting process.

3. Results and discussion

As can be seen in Figure 2, AWJM provided a high-quality surface finish on the samples, reducing or eliminating the need for secondary processes. The photographs in Figure 2 show the results of the coarse and fine cutting of the basalt fibre reinforced epoxy composite. Although the examples show that both cuts produce a high-quality cut, the main problem encountered in machining composites is the delamination that occurs during the cutting process [5].

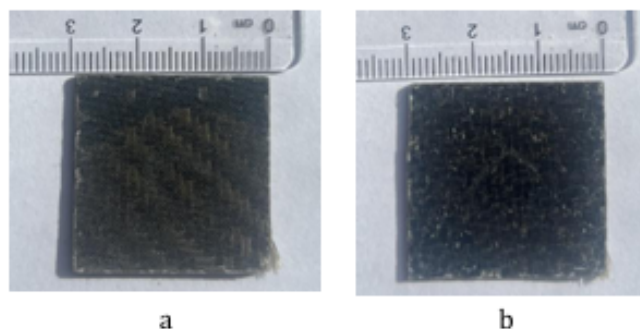


Fig. 2. Images of BFRPC samples: a - coarse cut and b - fine cut

The microscopic view of delamination of the samples is shown in Figure 3: coarse cutting (Fig. 3a), and fine cutting (Fig. 3c). It can be seen that the delamination occurred on the edge from which the cutting process started. The investigations of Shanmugam *et al.* [5] show that the delamination is caused by a shock wave caused by a water jet and the abrasive particles used in the cutting process. In addition, composites without good adhesion between the matrix and the reinforcing fibre are prone to defects such as cracks and delamination.

The cross-sectional surface images obtained from the optical microscope make it easy to identify the individual layers of the plays and the interface between them. Optical microscope images show that coarse cutting produces fractures and misalignments in the fibres (Fig. 3 b). The dark areas with small granular structures are the matrix region, which looks rough and uneven. There is also a visible gap between the fiber and the matrix (Fig. 3 b). In the case of fine cutting (Fig. 3d), less fiber breakage is visible compared to coarse cutting. The matrix region is also more compacted. Fine cutting samples show low fiber pull-out and more fiber matrix bonding. The alignment of the fibers is also more parallel and cleaner. In coarse cutting, microcracks are more present than in fine cutting.

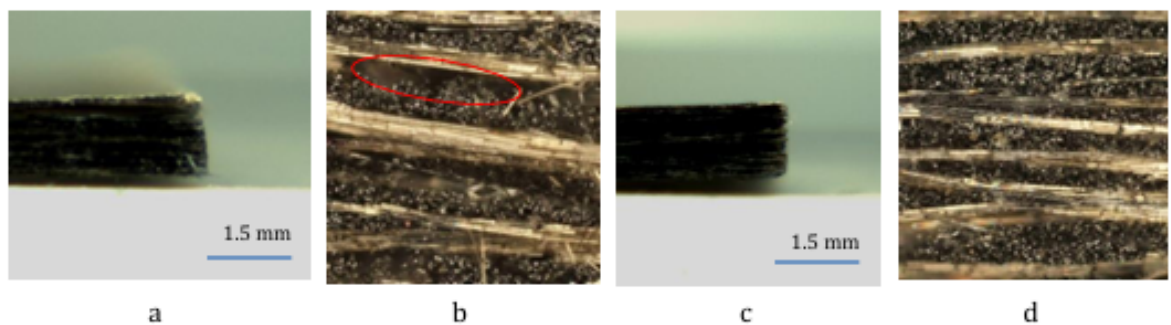


Fig. 3 Optical microscope images of BFRPC samples delamination: a- coarse cutting, c - fine cutting and images of BFRPC cross-sections at magnification $\times 10$: b - coarse cutting), b - fine cutting

The cross-sectional profiles presented in Figure 4 illustrate the surface profile of BFRPC after the coarse and fine cutting processes. In the coarse cutting profile, a very large difference between the peaks and valleys is clearly visible in some regions. This indicates that the surface is less smooth and rougher after coarse cutting. Sharp peaks and deep valleys are visible in the profile, which may be due to the effect of fiber pull-out or delamination during the cutting process. The increase in feed rate compared to fine cutting can be the reason for a more aggressive cutting action. The fine cutting profile shows high fluctuation, which means strong irregularities in the cut profile.

Fine cutting with a feed rate of 10 mm/min is supposed to be normal cutting with minimal damage, but the profilogram shows a result of a higher level of irregularities for a low feed rate.

From the details given in Table 1 on the roughness values. Normally, the values of R_a and R_q were expected to be lower for fine cutting compared to coarse cutting, but in this situation the results were the opposite of what was expected.

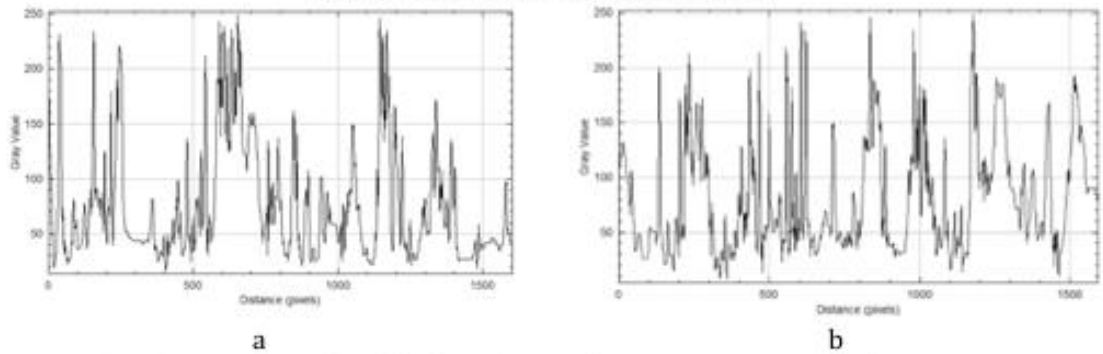


Fig. 4 Cross-sectional profile of BFRPC samples: a - coarse cutting; b - fine cutting

Table 1. Surface roughness values of coarse and fine cutting samples.

Cutting type	R_q (μm)	R_a (μm)
Coarse (22 mm/min)	57.240	30.63
Fine (10 mm/min)	59.372	32.95

However, the kerf angle values of both cuts show that the value of the kerf angle increased more than twice, then the feed rate increases from 10 mm/min to 22 mm/min (Fig. 5). During the cutting, the energy distributed from the water jet varies from top to bottom of the specimen. On top, the energy will be higher, which causes more material removal, and at the bottom, the energy distribution decreases gradually, resulting in taper angles. At higher feed rates, the jet nozzle moves faster, reducing the interaction time and the chances of cutting through the material completely, especially at the bottom, resulting in a wider cut at the top and a narrower cut at the bottom [6]. Studies by other researchers showed that a cone profile is formed at high feed rates and a reverse cone at low feed rates. The Kerf profile can be uniform and parallel at the optimum feed rate [7].



Fig. 5 The kerf angles of BFRPC: a - coarse cutting and b - fine cutting

Conclusions

The results obtained clearly demonstrate that AWM is an appropriate method for the machining of BFRPC.

1. Analysis of the roughness parameters showed that a low feed rate of 10 mm/min resulted in slightly higher roughness values compared to a feed rate of 22 mm/min.
2. The delamination of the cut surfaces was not affected by increasing the feed rate from 22 mm/min to 10 mm/min. The presence of delamination was obtained at the starting point of the composite cut due to the shock wave caused by a water jet and the abrasive particles used

in the cutting process, and the insufficient interfacial adhesion between the epoxy matrix and the basalt fibres.

3. The analysis of the angles showed that the low feed rate of 10 mm/min resulted in smaller angles and fewer defects compared to the feed rate of 22 mm/min, indicating that improved cut quality is achieved with lower feed rates.

References

1. BHONG, M., et al, 2023. Review of Composite Materials and Applications. *Materials Today: Proceedings*.
2. DHAND, V., et al, 2015. A Short Review on Basalt Fiber Reinforced Polymer Composites. *Composites Part B: Engineering*, vol. 73, pp. 166–180.
3. BINAZ, V., DEEPAK, K. and SINGH, I., 2023. Comparative Assessment of Cutting Processes in the Mechanical Behavior of Basalt Fiber/Poly (Lactic Acid) Matrix Composites. *Express Polymer Letters*, vol. 17, no. 2, pp. 152–168.
4. NATARAJAN, Y., MURUGESAN, P.K., MOHAN, M. and KHAN, S.A.L.A., 2020. Abrasive Water Jet Machining Process: A State of Art of Review. *Journal of Manufacturing Processes*, vol. 49, pp. 271–322.
5. SHANMUGAM, D.K., NGUYEN, T. and WANG, J., 2008. A Study of Delamination on Graphite/Epoxy Composites in Abrasive Waterjet Machining. *Composites Part A: Applied Science and Manufacturing*, vol. 39, no. 6, pp. 923–929.
6. KARKALOS, N.E., DEKSTER, L., KUDELSKI, R. and KARMIRIS-OBRAŃSKI, P., 2023. A Statistical and Optimization Study on the Influence of Different Abrasive Types on Kerf Quality and Productivity during Abrasive Waterjet (AWJ) Milling of Ti-4Al-6V. *Materials*, vol. 17, no. 1, pp. 11.
7. KHAN, M.A., SONI, H., MASHININI, P.M. and UTHAYAKUMAR, M., 2021. Abrasive Water Jet Cutting Process Form Machining Metals and Composites for Engineering Applications: A Review. *Engineering Research Express*, vol. 3, no. 2, pp. 022004.